

1 Effects of past climate variability on fire and vegetation in the cerrão savanna of the  
2 Huanchaca Mesetta, NE Bolivia  
3 S. Yoshi Maezumi<sup>1,2</sup>, Mitchell J. Power<sup>1,2</sup>, Francis E. Mayle<sup>3</sup>, Kendra McLauchlan<sup>4</sup>, José  
4 Iriarte<sup>5</sup>

5  
6 <sup>1</sup> Department of Geography, University of Utah, 260 S. Central Campus Dr., Rm: 270,  
7 Salt Lake City, UT 84112, USA

8 <sup>2</sup> Natural History Museum of Utah, 301 Wakara Way, Salt Lake City, UT 84103, USA

9 <sup>3</sup> Department of Geography and Environmental Science, Centre for Past Climate Change,  
10 University of Reading, Whiteknights, PO Box 227, Reading RG6, UK

11 <sup>4</sup> Department of Geography, Kansas State University, 118 Seaton Hall, Manhattan, KS  
12 66506, USA

13 <sup>5</sup> Department of Archaeology, College of Humanities, University of Exeter, Laver  
14 Building, North Park Road, Exeter EX4 4QE, UK

15  
16 Keywords: savanna, cerrão, *Mauritia flexuosa*, edaphic, climate, Holocene, fire,  
17 charcoal, stable isotopes, phytoliths, carbon, nitrogen, C<sub>3</sub> and C<sub>4</sub> grasses, South American  
18 Summer Monsoon, *surazos*

19  
20 Corresponding Author: [shira.maezumi@gmail.com](mailto:shira.maezumi@gmail.com), 001-(760)-212-6613

## 21 22 **Abstract**

23 *Cerrão* savannas have the greatest fire activity of all major global land-cover types  
24 and play a significant role in the global carbon cycle. During the 21<sup>st</sup> century,  
25 temperatures are projected to increase by ~3 °C coupled with a precipitation decrease of  
26 ~20%. Although these conditions could potentially intensify drought stress, it is unknown  
27 how that might alter vegetation composition and fire regimes. To assess how Neotropical  
28 savannas responded to past climate changes, a 14,500-year, high-resolution, sedimentary  
29 record from Huanchaca Mesetta, a palm swamp located in the *cerrão* savanna in  
30 northeastern Bolivia, was analyzed with phytoliths, stable isotopes and charcoal. A non-  
31 analogue, cold-adapted vegetation community dominated the Lateglacial-early Holocene  
32 period (14,500-9000 ka), that included trees and C<sub>3</sub> Pooideae and C<sub>4</sub> Panicoideae grasses.  
33 The Lateglacial vegetation was fire sensitive and fire activity during this period was low,  
34 likely responding to fuel availability and limitation. Although similar vegetation  
35 characterized the early Holocene, the warming conditions associated with the onset of the  
36 Holocene led to an initial increase in fire activity. Huanchaca Mesetta became  
37 increasingly fire-dependent during the middle Holocene with the expansion of C<sub>4</sub> fire  
38 adapted grasses. However, as warm, dry conditions, characterized by increased length  
39 and severity of the dry season, continued, fuel availability decreased. The establishment  
40 of the modern palm swamp vegetation occurred at 5000 cal yr BP. Edaphic factors are the  
41 first order control on vegetation on the rocky quartzite mesetta. Where soils are  
42 sufficiently thick, climate is the second order control of vegetation on the mesetta. The  
43 presence of the modern palm swamp is attributed to two factors: 1) increased  
44 precipitation that increased water table levels, and 2) decreased frequency and duration of  
45 *surazos* (cold wind incursions from Patagonia) leading to increased temperature minima.  
46 Natural (soil, climate, fire) drivers rather than anthropogenic drivers control the

47 vegetation and fire activity at Huanchaca Mesetta. Thus the *cerrado* savanna ecosystem  
48 of the Huanchaca Plateau has exhibited ecosystem resilience to major climatic changes in  
49 both temperature and precipitation since the Lateglacial period.  
50

## 51 **1. Introduction**

52 The *cerrado* savanna of central South America is the largest, richest, and likely most  
53 threatened savanna in the world (Da Silva Meneses and Bates 2002) The *cerrado* is the  
54 second largest biome in South America covering 1.86 million km<sup>2</sup> and is home to over  
55 10,000 plant species (Myers et al. 2000). The tropical forest-savanna ecotones within the  
56 *cerrado* biome are of considerable interest to biologists because of their high habitat  
57 heterogeneity (*beta* diversity), importance in rainforest speciation (Russell-Smith et al.  
58 1997) and sensitivity to climate change (IPCC 2014). According to current estimates  
59 however, only 20% of the *cerrado* remains undisturbed and only 1.2% of the area is  
60 preserved in protected areas (Mittermeier et al. 1999). Additionally, *cerrado* savannas  
61 have a significant role in the modern global carbon cycle because of high CO<sub>2</sub> loss  
62 associated with frequent natural fire activity (Malhi et al. 2002). Currently savanna fires  
63 are considered the largest source of natural pyrogenic emissions, with the most fire  
64 activity of all major global land cover types (Pereira 2003). In the last few decades,  
65 deforestation for agriculture and increased drought have resulted in increased burning in  
66 savannas, contributing to approximately 12% of the annual increase in atmospheric  
67 carbon (Van der Werf et al. 2010).

68 The *cerrado* biome comprises forest, savanna, and campestre (open field) formations  
69 (Mistry 1998, Abreu et al. 2012). *Cerrado sensu stricto* is characterized as a woody  
70 savanna formation composed of dense, thin, and rocky outcrops with *cerrado*  
71 physiognomies that are distinguishable based on their densities, heights, and scattered  
72 tree-shrub covers with roughly 50% trees and 50% grass (Abreu et al. 2012). The  
73 principal determinants of the growth and development of the *cerrado* vegetation types are  
74 largely related to edaphic factors (Colgan et al. 2012). For example the distribution of  
75 major *cerrado* vegetation types are closely related to the geomorphology of the  
76 Precambrian Brazilian shield in South America (Killeen 1998a). The development of the  
77 variety of *cerrado* vegetation communities is largely the result of heterogeneous nature of  
78 the edaphic features (Killeen 1998a) including the depth of the water table, drainage, the  
79 effective depth of the soil profile, the presence of concretions (Haridasan 2000), soil  
80 texture and the percentage of exposed rock (Junior and Haridasan 2005).

81 In addition to edaphic constraints, climate also has a prominent role in determining  
82 *cerrado* savanna vegetation structure and fire activity (Ribeiro and Walter 2008). The  
83 *cerrado* biome is dominated by a warm, wet-dry climate associated with the seasonal  
84 migration of the Intertropical Convergence Zone (ITCZ) (Da Silva Meneses and Bates  
85 2002, Vuille et al. 2012, Latrubesse et al. 2012). On synoptic climatological timescales,  
86 temperature and precipitation are the most important effects of climate on fire (e.g.  
87 months to seasons to years) (Mistry 1998). These factors govern net primary productivity  
88 (NPP) and the abundance of available fuels (Brown and Power 2013, Marlon et al. 2013).  
89 Warmer temperatures are typically associated with increased burning through vegetation  
90 productivity and the occurrence of fire-promoting climatic conditions. However, the role  
91 of temperature can be mediated by precipitation (Brown and Power 2013). Fire responds  
92 differently to increases in precipitation depending on whether fuel is initially abundant or

93 limited in the ecosystem (Mistry 1998, Marlon et al. 2013). In arid and semi-arid  
94 environments, such as the *cerrado*, increases in precipitation tend to increase fire,  
95 whereas increased precipitation in humid environments can reduce fire (Marlon et al.  
96 2008, 2013).

97 The seasonality of the precipitation coupled with abundant wet-season lightning  
98 ignitions (Ramos-Neto and Pivello 2000) is linked to high fire frequency in the *cerrado*  
99 (Miranda et al. 2009). Wet season lightning fires typically start in open vegetation (wet  
100 fields or grassy savannas) with significantly higher incidence of fire in more open  
101 savanna vegetation (Ramos-Neto and Pivello 2000). High biomass production during the  
102 wet season results in abundant dry fuels favoring frequent fires throughout the year  
103 (Ramos-Neto and Pivello 2000). Data show a positive correlation with fine fuel build-up  
104 and both fire temperature and fire intensity (energy output) (Fidelis et al. 2010). Thus,  
105 increased wet season fuel accumulation in the *cerrado* increases fire intensity. Based on  
106 an ecosystems adaptation to fire it can be classified as independent, fire-sensitive, and  
107 fire-dependent (Hardesty et al. 2005). In fire-independent ecosystems such as tundra and  
108 deserts, fire is rare, either because of unsuitable climate conditions or lack of biomass to  
109 burn. Fire-sensitive ecosystems such as tropical rainforests, are damaged by fire, which  
110 disrupts ecological processes that have not evolved with fire (Hardesty et al. 2005). Fire-  
111 dependent systems such as the well-drained grasslands of the *cerrado* biome, have  
112 evolved in the presence of periodic or episodic fires and depend on fire to maintain their  
113 ecological processes (Hardesty et al. 2005). Fire-dependent vegetation is fire-adapted,  
114 flammable and fire-maintained (Miranda et al. 2009, Pivello 2011).

115 The study of fire and vegetation change in the *cerrado* is increasingly important as  
116 population, agricultural activity, and global warming create pressing management  
117 challenges to preserve these biodiverse ecosystems (Mistry 1998). The long-term role of  
118 humans on vegetation and fire regimes of the *cerrado* remains unclear. During the late  
119 Holocene (3000 cal yr BP) there is increasing evidence for the increase in *Mauritia*  
120 *flexuosa* (*M. flexuosa*) and fire activity in Bolivia, Colombia, Venezuela and Brazil that  
121 has been attributed to both natural and anthropogenic drivers (Kahn and de Castro 1985,  
122 Kahn 1987, 1988, Behling and Hooghiemstra 1999, Berrio et al. 2002a, Rull 2009,  
123 Montoya and Rull 2011, Da Silva Meneses et al. 2013).

124 To investigate the drivers of vegetation and fire in the *cerrado* a long-term  
125 perspective is needed. The past few decades have experienced increased global  
126 temperatures, increased atmospheric CO<sub>2</sub>, and unprecedented levels of deforestation  
127 (Malhi et al. 2002). These recent changes heavily influence modern ecological studies,  
128 thus limiting the understanding of the role of natural variability in these systems. Long-  
129 term paleoecological studies can provide baseline information on processes shaping  
130 forest-savanna fire-vegetation dynamics from centennial-to-millennial timescales (Mayle  
131 and Whitney 2012). These long-term studies can inform whether recent shifts in ecotones  
132 are the result of a minor short-term oscillation around a relatively stable ecotone or a  
133 longer-term (e.g. millennial scale) unidirectional ecotonal shift forced by climate change  
134 (Mayle et al. 2000; Mayle and Whitney 2012). Additionally, long-term paleoecological  
135 records help form realistic conservation goals and identify fire management strategies for  
136 the maintenance or restoration of a desired biological state (Willis et al. 2007).

137 In this study, the long-term paleoecological perspective provides a context for  
138 understanding the role of centennial to millennial climate variability in the evolution of

139 fire and vegetation in *cerrado* savanna ecosystems. The purpose of this research is to  
140 explore long-term environmental change of *cerrado* savanna palm swamps in Bolivia  
141 from the Lateglacial (ca. 15,000 cal yr BP) to present. Paleoecological proxies including  
142 lithology, magnetic susceptibility, loss on ignition (LOI), charcoal, stable isotope, and  
143 phytolith data are used to investigate long-term ecosystem processes in the *cerrado*  
144 savanna. There are three primary hypotheses investigated in this study:

145

146 (1) Edaphic conditions are the dominant control on the presence of savanna versus  
147 forest vegetation on the Huanchaca Mesetta.

148 (2) Climate is the dominant control on savanna structure and floristic composition.

149 (3) The late Holocene rise in *M. flexuosa* was driven by climate rather than a change  
150 in human land-use.

151

### 152 1.1 Study Site

153 Noel Kempff Mercado National Park (NKMNP), a 15,230 km<sup>2</sup> biological reserve in  
154 northeastern Bolivia, is located on the Precambrian Shield near the southwestern margin  
155 of the Amazon Basin, adjacent to the Brazilian States of Rondônia and Mato Grosso  
156 (Burbridge et al. 2004). It is a UNESCO World Heritage Site, in recognition of its  
157 globally important biodiversity and largely undisturbed ecosystems, including *terra firme*  
158 (non-flooded) evergreen rainforest, riparian and seasonally-flooded humid evergreen  
159 forest, seasonally flooded savanna, wetlands, upland *cerrado* savannas, and semi-  
160 deciduous dry forests (Mayle et al. 2007). NKMNP occupies an ecotone between  
161 Amazon rainforest to the north and dry forests and savannas to the south, containing 22  
162 plant communities (Figure 1) (Burn et al. 2010). Huanchaca Mesetta palm swamp  
163 (14°32'10.66"S, 60° 43'55.92"W, elevation: 1070 m a.s.l.) is located within NKMNP on  
164 the Huanchaca Mesetta – an 800-900 m elevation table mountain. The palm swamp is  
165 approximately 200 by 50 meters, comprised entirely of a mono-specific stand of the palm  
166 *M. flexuosa*.

167

### 168 1.2 Climate

169 The climate of NKMNP is characterized by a tropical wet and dry climate (Da Silva  
170 Meneses and Bates 2002). The mean annual precipitation at NKMNP derived from  
171 nearby weather stations (Concepción, Magdalena, San Ignacio) is ca. 1400-1500 mm per  
172 year, with mean annual temperatures between 25 and 26 °C (Hanagarth, 1993; Montes de  
173 Oca, 1982; Roche and Rocha, 1985). There is a three to five month dry season during the  
174 Southern Hemisphere winter (May to September-October), when the mean monthly  
175 precipitation is less than 30 mm (Killeen 1990). Precipitation falls mainly during the  
176 austral summer (December to March), originating from a combination of deep-cell  
177 convective activity in the Amazon Basin from the South American Summer Monsoon  
178 (SASM) and the ITCZ (Vuille et al. 2012). The SASM transports Atlantic moisture into  
179 the basin and corresponds to the southern extension of the ITCZ. The ITCZ is driven by  
180 seasonal variation in insolation; thus, maximum southern hemisphere insolation and  
181 precipitation occur in the austral summer (Bush and Silman 2004, Vuille et al. 2012).  
182 During winter (June, July, August), cold, dry polar advections from Patagonia, locally  
183 known as *surazos*, can cause short-term cold temperatures to frequently decrease down to  
184 10 °C for several days at a time (Mayle and Whitney 2012, Latrubesse et al. 2012). These

185 abrupt decreases in temperature may potentially influence the distribution of temperature-  
186 limited species on the Huanchaca Mesetta.

187

### 188 1.3 Geomorphology

189 The Huanchaca Mesetta table mountain is near the western limit of the Brazilian  
190 Shield and dominates the eastern half of NKMNP. It is composed of Precambrian  
191 sandstone and quartzite (Litherland and Power 1989). The top of the mesetta is flat, with  
192 a gently rolling surface and at elevations ranging from 500-900 m above sea level (a.s.l.)  
193 (Da Silva Meneses and Bates 2002). The substrate of the mesetta is rocky, and soils are  
194 thin and low in organic material (Litherland and Power 1989). Continuity of the  
195 crystalline or sedimentary blocks of the mesetta is broken by an extensive network of  
196 peripheral or inter-mesetta depressions formed from a combination of erosion, dolerite  
197 dike intrusions and faulting on the mesetta (Litherland and Power 1989, Da Silva  
198 Meneses and Bates 2002). These depressions act as catchments for sediment and water,  
199 resulting in sediment accumulation, which supports more complex vegetation  
200 communities. High species diversity exhibited on the Huanchaca Mesetta, compared  
201 with other savanna regions of South America, is attributed to the long history of isolation  
202 of this edaphically-controlled table-mountain savanna (Mayle et al. 2007).

203

### 204 1.4 Vegetation

205 The *cerrado* savanna on Huanchaca Mesetta is dominated by a continuous grass  
206 cover with sparsely scattered small trees and shrubs that grows on the thin, well-drained,  
207 nutrient-poor soils (Killeen 1998b). Woody species include *Byrsonima coccolobifolia*,  
208 *Caryocar brasiliensis*, *Erythroxylum suberosum*, *Vochysia haenkeana*, and *Callisthene*  
209 *fasciculata*. Trees and shrubs include *Qualea multiflora*, *Emmotum nitens*, *Myrcia*  
210 *amazonica*, *Pouteria ramiflora*, *Diptychandra aurantiaca*, *Kielmeyera coriacea*, *Ouratea*  
211 *spectabilis*, and *Alibertia edulis*. Small-shrubs include *Eugenia punicifolia*, *Senna*  
212 *velutina*, and herbaceous species include *Chamaecrista desvauxii*, and *Borreria sp.*  
213 Monocot families include the Rapateaceae (C<sub>3</sub>) (*Cephalostemon microglochis*),  
214 Orchidaceae (*Cleistes paranaensis*) (CAM, C<sub>3</sub>), Iridaceae (*Sisyrinchium* spp.) (C<sub>4</sub>),  
215 Xyridaceae (*Xyris* spp.) (C<sub>4</sub>), and Eriocaulaceae (*Eriocaulon* spp., *Paepalanthus* spp.,  
216 *Syngonanthus* spp.) (C<sub>4</sub>) (Killeen 1998b). In the inter-fluvial depressions organic rich soil  
217 is sufficiently deep to support humid evergreen forests islands which are typically  
218 dominated by mono-specific stands of *M. flexuosa* (Da Silva Meneses and Bates 2002,  
219 Mayle and Whitney 2012). *M. flexuosa* is a monocaulous, aborescent palm, averaging 20-  
220 30 meters tall which is typically associated with a low, dense understory (da Silva and  
221 Bates, 2002; Furley and Ratter, 1988; Kahn, 1988;). *M. f.* is confined to lower elevations  
222 (< ca. 1000 m elevation) in warm/wet climates (Rull and Montoya 2014). *M. flexuosa*  
223 swamps favor inter-fluvial depressions that remain flooded during the dry season, when  
224 the surrounding terrains dry out (Kahn and de Granville 1992, Huber 1995a, 1995b). The  
225 abundance of *M. flexuosa* in permanently flooded, poorly drained soils is the result of  
226 pneumatophores (aerial roots) which enable its growth in anaerobic conditions (Kahn  
227 1988, Rull and Montoya 2014). Seasonal water deficits saturate the soil profile in the wet  
228 season and desiccate soil during the dry season resulting in a dominance of herbaceous  
229 versus woody plants surrounding the inter-fluvial depressions (Killeen 1998b). The  
230 seasonal dryness leads to drought, plant water stress, and frequent fire activity resulting

231 in the development of xeromorphic and sclerophyllous plant characteristics on the open  
232 mesetta (Killeen 1998b). The spatial distribution of evergreen forest versus drought-  
233 tolerant savanna vegetation is additionally constrained by edaphic conditions limiting the  
234 expansion of forest vegetation because of the heavily weathered sandstone soils dominant  
235 outside the inter-fluvial depressions (Killeen and Schulenberg 1998). Limited soil  
236 development precludes rainforest from developing on the large, rocky expanses of the  
237 mesetta (Killeen and Schulenberg 1998). The essentially treeless campo *cerrado* that  
238 grows around Huanchaca Mesetta palm swamp is edaphically constrained and has likely  
239 grown on this mesetta for millions of years (Mayle and Whitney 2012). Thus, the  
240 vegetation of the Huanchaca Mesetta is influenced by both climatic and non-climatic  
241 controls including seasonal hydrologic conditions, edaphic soil constraints and frequent  
242 fire activity (Killeen and Schulenberg 1998).

243

## 244 **2 Materials & Methods**

### 245 *2.1 Sediment core*

246 A 5.48 m-long sediment core from Huanchaca Mesetta palm swamp was collected in  
247 1995 using a Livingstone modified square-rod piston corer from the center of the swamp.  
248 The uppermost 15 cm, containing a dense root mat, was discarded because of the  
249 presence of fibrous roots and potential for sediment mixing. Huanchaca Mesetta sediment  
250 cores were transported to the Utah Museum of Natural History for analysis. They were  
251 photographed and described using a Munsell soil color chart. Visual descriptions,  
252 including sediment type, structure, texture, and organic content were undertaken to assist  
253 interpretation of the palaeoenvironmental data.

254

### 255 *2.2 Chronology*

256 The chronological framework for Huanchaca Mesetta was based on eight accelerator  
257 mass spectrometry (AMS) radiocarbon dates from non-calcareous bulk sediment and  
258 wood macrofossils analyzed at the University of Georgia Center for Applied Isotope  
259 Studies (Table 1). The uncalibrated radiometric ages are given in radiocarbon years  
260 before 1950 AD (years ‘before present’, yr BP). Radiocarbon ages were calibrated using  
261 CALIB 7.0 and the IntCal13 calibration dataset (Reimer et al. 2013). IntCal13 was  
262 selected in place of the SHcal13 calibration curve because of the latitudinal location  
263 (14°S) of Huanchaca Mesetta and the proximal hydrologic connection with the origin of  
264 the South American Monsoon in the northern hemisphere. The seasonal migration of the  
265 ITCZ is thought to introduce a northern hemisphere <sup>14</sup>C signal to the low latitude  
266 southern hemisphere (McCormac et al. 2004). This study area is located in the low  
267 latitudes (14°S) and within the range of the ITCZ migration; thus, the IntCal13  
268 calibration curve was selected for the radiocarbon calibrations. Following calibration, the  
269 mean age value of calibrated years before present (cal yr BP) of the largest probability at  
270 2 sigma standard deviation was used to reflect both statistical and experimental errors)  
271 (grey bars in Figure 2). These mean ages were used to create the smoothing spline age  
272 model using classical age-depth modeling, in the package CLAM (Blaauw 2010) within  
273 the open-source statistical software R.

274

275

276

277

### 278 *2.3 Loss on Ignition*

279 The variability in the organic and carbonate content of sediments is used, in  
280 conjunction with magnetic susceptibility, to identify periods of variability in sediment  
281 composition and organic content throughout the Holocene. Organic and carbonate  
282 sediment composition was determined by Loss-on-Ignition (LOI), conducted at  
283 contiguous 1 cm increments throughout the cores. For each sample, 1 cm<sup>3</sup> of sediment  
284 was dried in an oven at 100°C for 24 hours. The samples underwent a series of 2-hour  
285 burns in a muffle furnace at 550°C and 1000°C to determine the relative percentage of the  
286 sample composed of organics and carbonates. Concentration was determined by weight  
287 following standard methodology (Dean Jr 1974).

288

### 289 *2.4 Magnetic Susceptibility*

290 Magnetic susceptibility (MS) was measured to identify mineralogical variation in the  
291 sediments (Nowaczyk 2001). The MS of sediments is reflective of the relative  
292 concentration of ferromagnetic (high positive MS), paramagnetic (low positive MS), and  
293 diamagnetic (weak negative MS) minerals or materials. Typically, sediment derived from  
294 freshly eroded rock has a relatively high MS, whereas sediments that are dominated by  
295 organic debris, evaporites, or sediments that have undergone significant diagenetic  
296 alteration typically have a low or even negative MS (Reynolds et al. 2001). Shifts in the  
297 magnetic signature of the sediment can be diagnostic of a disturbance event (Gedye et al.  
298 2000). Sediment cores were scanned horizontally, end to end through the ring sensor.  
299 MS was conducted at 1 cm intervals using a Barington ring sensor equipped with a 75  
300 mm aperture.

301

### 302 *2.5 Charcoal*

303 Sediment samples were analyzed for charcoal pieces greater than 125 µm using a  
304 modified macroscopic sieving method (Whitlock and Larsen 2001) to reconstruct the  
305 history of local and extra-local fires. Charcoal was analyzed in contiguous 0.5 cm  
306 intervals for the entire length of the sediment core at 1 cm<sup>3</sup> volume. Samples were  
307 treated with 5% potassium hydroxide in a hot water bath for 15 minutes. The residue was  
308 gently sieved through a 125 µm sieve. Macroscopic charcoal (particles >125 µm in  
309 minimum diameter) was counted in a gridded petri dish at 40× on a dissecting  
310 microscope. Non-arboreal charcoal was characterized by two morphotypes: (1) cellular  
311 'graminoid' (thin rectangular pieces; one cell layer thick with pores and visible vessels  
312 and cell wall separations) and (2) fibrous (collections or bundles of this filamentous  
313 charcoal clumped together). Arboreal charcoal was characterized by three morphotypes:  
314 (1) dark (opaque, thick, solid, geometric in shape, some luster, and straight edges), (2)  
315 lattice (cross-hatched forming rectangular ladder-like structure with spaces between) and  
316 (3) branched (dendroidal, generally cylindrical with successively smaller jutting arms)  
317 (Jensen et al. 2007, Tweiten et al. 2009, Mueller et al. 2014). Charcoal pieces were  
318 grouped into non-arboreal and arboreal categories based on their morphology, which  
319 enabled the characterization of fuel sources in the charcoal record (Mueller et al. 2014).

320 Charcoal counts were converted to charcoal influx (number of charcoal particles cm<sup>-2</sup>  
321 <sup>3</sup>) and charcoal influx rates by dividing by the deposition time (yr cm<sup>-1</sup>) using CHAR  
322 statistical software (Higuera et al. 2009). In CHAR, charcoal data was decomposed to

323 identify distinct charcoal peaks based on a standard set of threshold criteria. Low  
324 frequency variation is considered background charcoal which reflect changes in the rate  
325 of total charcoal production, secondary charcoal transport and sediment mixing (Higuera  
326 et al. 2007). If the charcoal data exceed that background threshold, it is considered a peak  
327 and interpreted here as a fire episode. Background was calculated using a 700-yr moving  
328 average.

329

## 330 2.6 Stable Isotopes

331 Stable carbon isotopes were analyzed as an additional proxy for changes in vegetation  
332 structure and composition. Carbon isotopic composition of terrestrial organic matter is  
333 determined primarily by the photosynthetic pathway of vegetation (Malamud-Roam et al.  
334 2006). Previous research on  $\delta^{13}\text{C}$  values of the Huanchaca Mesetta have been used to  
335 determine the relative proportions of  $\text{C}_4$  savanna grasses versus  $\text{C}_3$  woody and herbaceous  
336 vegetation (Killeen et al., 2003; Mayle, Langstroth, Fisher, & Meir, 2007).

337 Sediment  $\delta^{15}\text{N}$  integrates a variety of nutrient cycling processes including the loss of  
338 inorganic N to the atmosphere through denitrification (Robinson 1991, McLauchlan et al.  
339 2013). Denitrification and the subsequent enrichment of  $\delta^{15}\text{N}$  requires abundant available  
340 carbon, available nitrate, and anaerobic conditions (Seitzinger et al. 2006). Thus, wet,  
341 anoxic soils tend to have enriched values of  $\delta^{15}\text{N}$ . Environmental conditions that alter  
342 from wet (anaerobic) to dry (aerobic) conditions also enrich  $\delta^{15}\text{N}$  values (Codron et al.  
343 2005). During dry periods, denitrification is shut off because of an increase in available  
344 oxygen in sediments, thus  $\delta^{15}\text{N}$  values decrease. If dry soils become hydrated, there is a  
345 preferential loss of  $^{14}\text{N}$ , enriching  $\delta^{15}\text{N}$  values (Codron et al. 2005). Stable isotope  
346 analysis was conducted at 3-cm resolution for total carbon (C) and nitrogen (N)  
347 throughout the length of the sediment core. One  $\text{cm}^3$  of bulk sediment was dried,  
348 powdered, and treated with 0.5 molar hydrochloric acid to remove carbonates. A range of  
349 1-25 mg of the dried carbonate-free sediment was weighed into tin capsules depending on  
350 organic matter content. The samples were analyzed on a Finnigan Delta dual inlet  
351 elemental analyzer at the Sirfer Lab at the University of Utah.  $^{13}\text{C}/^{12}\text{C}$  and  $^{15}\text{N}/^{14}\text{N}$  ratios  
352 are presented in delta ( $\delta$ ) notation, in per mil ( $^0/_{00}$ ) relative to the PDB and  $\text{N}_2$  air  
353 standards) (Codron et al. 2005).

354

## 355 2.7 Phytoliths

356 Phytoliths preserve well in sediment records and are especially useful in areas with  
357 intermittent dry periods. Phytoliths were used as a proxy to reconstruct past vegetation  
358 composition and are especially useful in the lower taxonomic identification of grasses  
359 (Piperno and Pearsall 1998). Grass phytoliths can provide important paleoecological  
360 information. Tropical  $\text{C}_4$  grasses, adapted to open environments with high seasonality of  
361 rainfall, typically expand at the expense of  $\text{C}_3$  grasses and other tropical forest species  
362 during drier intervals (Hartley 1958a, 1958b, Hartley and Slater 1960, Piperno 1997).  $\text{C}_4$   
363 Panicoideae grasses are generally adapted to warm moist conditions, whereas  $\text{C}_4$  Chloride  
364 grasses are adapted to warm, dry conditions (Hartley and Slater 1960).  $\text{C}_3$  subfamilies,  
365 including the Pooideae, are adapted to cool and moist conditions, are currently confined  
366 to temperate climates with lower temperatures (Hartley 1961, 1973, Iriarte 2006). The  
367 presence of  $\text{C}_3$  Pooideae grasses from phytolith data from southeastern Pampa grasslands  
368 in Uruguay have been interpreted to indicate a shorter dry season with overall conditions



369 that were cooler than during the Holocene (Iriarte 2006). Phytolith samples were taken  
370 every 4 cm along the sediment core. The extraction and slide preparation of phytoliths  
371 were conducted at the University of Exeter, UK, following standard procedures described  
372 by Piperno (2005). Slides were scanned and counted at the University of Utah Power  
373 Paleocology Lab using a Leica EMED compound light microscope (400-1000x). The  
374 number of phytoliths counted varied from 101-320 per slide. The modern palm swamp is  
375 a monospecific stand of *M. flexuosa* that produces globular echinate phytoliths but does  
376 not produce hat-shaped phytoliths characteristic of other Arecaceae (Piperno 2005).  
377 Although other palms produce globular echinate phytoliths, the current monospecific  
378 stand supports the identification of globular echinate phytoliths as belonging to this palm.

379 Given the abundance of *M. flexuosa* during the middle and late Holocene, phytolith  
380 percentages from globular echinate phytoliths were calculated separately. Percentages of  
381 non-*Mauritia* phytoliths were calculated on the basis of the total sum of phytoliths  
382 excluding *M. flexuosa*. Phytolith identification was made by comparison with modern  
383 plant reference collections curated at the University of Exeter Archaeobotany Lab. The  
384 classification of Poaceae implemented a three-partite morphological classification related  
385 to grass taxonomy (Panicoideae-Chloridoideae-Pooideae) (Twiss et al. 1969) and further  
386 developed in both North America (Fredlund and Tieszen 1994) and the Neotropics  
387 (Sendulsky and Labouriau 1966, Söndahl and Labouriau 1970, Teixeira da Silva and  
388 Labouriau 1970, Bertoli de Pomar 1971, Zucol 1999, 2000, 1996, 1998, Piperno and  
389 Pearsall 1998, Iriarte 2003, Piperno 2005, Iriarte and Paz 2009). The phytolith percentage  
390 diagrams were plotted using Tilia and Tilia Graphing software (Grimm 1987). CONISS  
391 was used to calculate phytolith zones (Grimm 1987). CONISS is based on cluster  
392 analysis, with the constrain that clusters are formed by hierarchical agglomeration of  
393 stratigraphically-adjacent samples (Grimm 1987, Bennett 1996) and a broken-stick model  
394 was used to determine statistically significant zones (Bennett 1996).

395

### 396 **3 Results**

397 Four distinct zones were identified including: Zone 1: the Lateglacial (14,500-11,800  
398 cal yr BP), Zone 2: the early Holocene (11,800-9000 cal yr BP), Zone 3: the middle  
399 Holocene (8000-3500 cal yr BP), and Zone 4a and 4b: the late Holocene (3500 cal yr BP  
400 to present).

401

#### 402 *3.1 Zone 1: 14,500-11,800 cal yr BP Lateglacial*

403

404 The Lateglacial vegetation on Huanchaca Mesetta was dominated by arboreal taxa,  
405 grasses and Asteraceae (Opaque Perforated platelets) phytoliths (Figure 3). The phytolith  
406 assemblage likely contains both in-situ vegetation production and wind-blown vegetation  
407 from the surrounding rocky savanna. Both C<sub>4</sub> Panicoideae and C<sub>3</sub> Pooideae grass  
408 phytoliths were present during the Lateglacial. The presence of C<sub>3</sub> Pooideae grasses is  
409 interpreted as cooler Lateglacial conditions compared to present. The Lateglacial  
410 vegetation community at Huanchaca Mesetta lacks a modern analogue plant community  
411 in NKMNP. The presence of both of C<sub>3</sub> Pooideae and C<sub>4</sub> Panicoideae grasses suggest  
412 some degree of landscape heterogeneity. A consistent layer of very dark sandy silt  
413 dominated the lithology of Huanchaca Mesetta during the Lateglacial. The magnetic  
414 susceptibility and bulk density values were low and exhibit minimum variability

415 compared to the rest of the record (Figure 4). Coupled with LOI organic values below  
416 10%, the sediment lithology was summarized as a low-energy depositional environment  
417 with relatively low nutrient input. Organic matter deposited during the Lateglacial had  
418  $\delta^{13}\text{C}$  values of -16‰ (Figure 5), indicating a contribution of  $\text{C}_4$  grasses to organic matter  
419 composition. The proportion of  $\text{C}_3$  to  $\text{C}_4$  grass contribution was calculated by using  
420 values of  $\text{C}_3$  and  $\text{C}_4$  grasses and a simple two-pool mixing model (Perdue and Koprivnjak  
421 2007) with end member values of -27‰ for  $\text{C}_3$  and -12‰ for  $\text{C}_4$  plants. The contribution  
422 of  $\text{C}_4$  vegetation was ca. 80%, higher than any other time in the Huanchaca record.  
423 Modern  $\delta^{13}\text{C}$  values in the basin range from -18 to -22‰. The location of these  $\text{C}_4$   
424 drought adapted grasses was likely the surrounding plateau. Organic carbon  
425 concentrations gradually increased from 1% to 4% during the Lateglacial, indicating  
426 relatively low amounts of organic matter in the system compared to those of today. The  
427 C:N ratio ranged from 20 to 30, indicating a terrestrial organic matter source. N  
428 concentrations were low from 0.1 to 0.2% and the  $\delta^{15}\text{N}$  values were ca. 5‰ indicating  
429 minimal denitrification during the Lateglacial. The  $\delta^{13}\text{C}$ , %  $\text{C}_4$  contribution, and high  
430 C:N values coupled with the phytolith data dominated by trees and grasses, suggest a  
431 predominantly terrestrial signal, characterized by an open savanna grassland during the  
432 Lateglacial (Figure 6). The  $\delta^{15}\text{N}$  values suggest that sediments within the swamp were  
433 drier than present creating aerobic conditions and low denitrification rates.

434 Charcoal influx levels were low during the Lateglacial (14,500-12,000 cal yr BP).  
435 Fire return interval (FRI) was 2 fire episodes per 1000 yr (Figure 7). Based on the 0.5 cm  
436 sampling resolution of this record, fire “episodes” were interpreted as periods of  
437 increased fire activity rather than isolated fire “event”. The charcoal signature was  
438 consistent with frequent, low intensity fires that likely occurred in the open, grass  
439 dominated mesetta surrounding the basin. Low charcoal influx levels coupled with low  
440 magnitude charcoal peaks, suggest that the non-analogue vegetation structure of  $\text{C}_3$   
441 Pooideae,  $\text{C}_4$  Panicoideae, and arboreal phytoliths likely created a fuel structure that  
442 lacked sufficient density or fuel connectivity to produce abundant arboreal or grass  
443 charcoal. Low charcoal influx coupled with low fire frequency suggest that the  
444 Lateglacial environment was likely fire-sensitive within the basin.

445

### 446 3.2 Zone 2: 11,800-9000 cal yr BP early Holocene

447

448 There were decreased  $\text{C}_4$  Panicoideae grasses, with consistent levels of  $\text{C}_3$  Pooideae  
449 grasses, arboreal, and Asteraceae (Opaque perforated platelets) phytoliths. The presence  
450 of  $\text{C}_3$  grasses, and the absence of *M. flexuosa*, the dominant component of the modern  
451 basin vegetation, suggest temperatures cooler than present. The lithology, magnetic  
452 susceptibility, bulk density, and LOI values indicate minimal shift during the vegetation  
453 transition. Organic geochemistry reflected a change in organic matter source, with  $\delta^{13}\text{C}$   
454 values becoming more negative, indicating an increase in the contribution of  $\text{C}_3$   
455 vegetation ca. 11,000 cal yr BP. The  $\delta^{13}\text{C}$  contribution of  $\text{C}_4$  grasses decreased  
456 dramatically from 60 to 20% during this period (Figure 8). These data correspond to a  
457 decrease in  $\text{C}_4$  Panicoideae grass phytoliths and an increase in arboreal phytoliths. Low  
458 levels of terrestrial organic input into the system were indicated by low carbon  
459 concentrations and C:N values ranging between 25 and 30. N cycling changed during  
460 this zone, with  $\delta^{15}\text{N}$  values exhibiting greater amplitude and higher frequency variability.

461 The  $\delta^{15}\text{N}$  values ranged between 4 and 8‰ indicating increased variability in  
462 denitrification rates associated with increasing wet (anaerobic) to dry (aerobic)  
463 conditions. The N concentrations were low, between 0.05 and 0.01%, indicating minimal  
464 nitrogen availability in the system.

465 Charcoal influx at Huanchaca Mesetta increased ca. 11,200 cal yr BP coupled with  
466 an increase in the fire frequency to 5 episodes (periods of increased burning) per 1000 yr.  
467 The peak magnitude values indicated two substantial fire episodes (periods of increased  
468 burning) ca. 10,200 and 9100 cal yr BP. The lack of significant change in the lithology  
469 suggests that taphonomic conditions were consistent during this interval. The increase in  
470 grass phytoliths during this period coupled with the increase in charcoal influx and fire  
471 episodes suggest that the early Holocene vegetation community was becoming  
472 increasingly more fire dependent and vegetation was likely adapting to the increase in  
473 fire frequency associated with the period.

474

### 475 3.3 Zone 3: 8000-3750 cal yr BP middle Holocene

476

477 Significant vegetation changes occur through the middle Holocene. From 8000 to  
478 5500 cal yr BP,  $C_4$  Panicoideae (warm/wet) grasses were at the lowest values in the  
479 record.  $C_3$  Pooideae (cold/wet) grasses diminished after ca. 7000 cal yr BP and remain  
480 absent for the remainder of the record. Arboreal phytoliths reached the highest levels in  
481 the record at 8000 cal yr BP followed by a slight decline to 3500 cal yr BP.  $\delta^{13}\text{C}$  values  
482 ranged between -24 and -22‰ from 7900 cal yr BP to 5100 cal yr BP. These values  
483 corresponded to a diminished  $C_4$  contribution to organic matter (approximately 18%).  
484 Decreased  $C_4$  grass phytoliths from 8000 to 5000 cal yr BP was interpreted as a decrease  
485 in vegetation density in the open mesetta surrounding the basin caused by drying  
486 conditions on the mesetta. After 5000 cal yr BP,  $C_4$  Panicoideae grasses and  $C_4$  Chloride  
487 (warm/dry) grasses gradually increased in the surrounding watershed, coupled increased  
488  $\delta^{13}\text{C}$  values to -19‰. *M. flexuosa* phytoliths first appeared at 5000 cal yr BP, and  
489 gradually increased to modern levels by 3750 cal yr BP. The  $\delta^{13}\text{C}$  values decreased,  
490 potentially associated with the development of the  $C_3$  *M. flexuosa* community. A dark-  
491 brown clay-sand mixture from 8000 to 3750 cal yr BP dominated the lithology that  
492 transitioned to black detrital peat ca. 3750 cal yr BP associated with the establishment of  
493 *M. flexuosa*. After 4000 cal yr BP LOI, magnetic susceptibility, and C:N values  
494 increased, indicating increased organic material. Nitrogen cycling continued to fluctuate  
495 throughout this period.  $\delta^{15}\text{N}$  values exhibited the greatest frequency and amplitude of  
496 variability from 8000 to 3750 cal yr BP ranging from 2 to 12‰ indicating repeated and  
497 extensive dry periods on the mesetta.

498 Increased charcoal influx ca. 8000 cal yr BP was followed by an abrupt decrease to  
499 the lowest values during the record from ca. 7900 to ca. 3800 cal yr BP. Peak frequency  
500 reached the highest levels of 6 fire episodes (periods of increased burning) per 1000 yr  
501 during the middle Holocene. These data corresponded to the highest levels of  $\delta^{15}\text{N}$  values  
502 indicating extended dry periods that likely promoted frequent fires on the mesetta. The  
503 first evidence of grass charcoal appeared ca. 6500 cal yr BP suggesting a change in the  
504 fire ecology on the mesetta. From 5000 to 3750 cal yr BP, grass charcoal increased. This  
505 is coincident with the establishment of *M. flexuosa* palm swamp and increased  $C_4$  grasses  
506 in the surrounding watershed. After 3900 cal yr BP, charcoal influx and fire frequency

507 increased. Significant increases in grass charcoal reflected a change in the fuel  
508 composition in the watershed. Phytolith, isotope and charcoal data suggest that after 3900  
509 cal yr BP, the *M. flexuosa* within the basin became increasingly fire-sensitive and the  
510 occurrence of a fire within the palm stand would have had consequences for the  
511 vegetation not adapted to fire. The fire adapted C<sub>4</sub> grass dominated watershed continued  
512 to be fire-dependent.

513

514

515 *3.4 Zone 4: 3750 to 2000 cal yr BP: late Holocene*

516

517 There is a decrease in arboreal taxa coupled with increased values of *M. flexuosa*. C<sub>4</sub>  
518 Panicoideae (warm, wet) grasses continued to dominate the surrounding watershed. The  
519 lithology consisted of black detrital peat ca. 2450-2050 cal yr BP associated with high  
520 LOI values (ca. 22 % organics) and magnetic susceptibility values (ca. 1000 10<sup>-5</sup> SI).  
521 After 2500 cal yr BP the %C, %N, and δ<sup>15</sup>N increased suggesting moist, anoxic  
522 conditions that enabled moderate denitrification from the swamp. These lithologic and  
523 isotopic data represented the establishment of modern palm swamp characterized by  
524 increased autochthonous organic accumulation. The δ<sup>13</sup>C values reached modern levels  
525 by 2800 cal yr BP although, values exhibit increased variability, fluctuating between -19  
526 and -24‰ co-varying with the C<sub>4</sub> grass contribution between 10-20%.

527 Charcoal influx at Huanchaca Mesetta remained low 3750 to 2000 cal yr BP with a  
528 FRI of 5 episodes (periods of increased burning) per 1000yrs. Grass charcoal reached the  
529 highest continuous levels ca. 2800 to 2000 corresponding to high levels of fire adapted C<sub>4</sub>  
530 grass phytoliths. Increased grass charcoal coupled with low peak magnitude values and  
531 high fire frequency indicated that the vegetation surrounding the palm swamp was fire  
532 dependent and fire adapted. However within the moist *M. flexuosa* palm stand, the  
533 vegetation remained fire sensitive.

534

535 *3.5 Zone 5: 2000 cal yr BP to Present: late Holocene*

536

537 *M. flexuosa* reached the highest levels in the record in ca. 1800 cal yr BP followed by  
538 decreasing values towards present. The presence of hat shaped phytoliths ca. 200 cal yr  
539 BP indicate very low concentrations of other palm species during this time. There was a  
540 gradual decrease in *M. flexuosa* towards present coupled with the highest levels of C<sub>4</sub>  
541 Panicoideae grasses ca. 200 cal yr BP and a decrease in C<sub>4</sub> Chloridoideae (warm, dry)  
542 grasses in the surrounding watershed. The lithology was dominated by dark brown  
543 detrital peat. After ca. 800 cal yr BP δ<sup>13</sup>C values were ca. -18‰ and the % C<sub>4</sub>  
544 contribution was ca. 50%. These data corresponded to the highest levels of C<sub>4</sub>  
545 Panicoideae grass phytoliths in the record. The dark detrital peat lithology was  
546 interrupted by two coarse sand layers ca. 1550 cal yr BP and ca. 300-200 cal yr BP,  
547 followed by a shift back to black detrital peat ca. 200 cal yr BP to present. These sand  
548 layers were characterized by a decrease in LOI from ca. 22 to 2 % organics, C:N ratios  
549 from ca. 25 to 0, and δ<sup>15</sup>N from ca. 5 to 0‰ coupled with increased magnetic  
550 susceptibility and bulk density values suggesting clastic flood events associated with  
551 sandy sediments low in organic material. From 300 cal yr BP %C values increased from  
552 ca. 1% to >20% reached the highest values in the record. The %N values increased from

553 ca. 01 to the peak Holocene values of 1.2 at present. The dramatic increases in both %C  
554 and %N were likely the result of in situ carbon cycling and nitrogen fixation.

555 Charcoal influx increased after 2000 cal yr BP at ca. 1400 to 1200 cal yr BP, and  
556 reached peak Holocene values ca. 500-400 cal yr BP. Increased charcoal was coupled  
557 with the lowest FRI values in the record. Peak magnitude increased significantly around  
558 1200 cal yr BP and the largest peak magnitude values ca. 200 cal yr BP. These charcoal  
559 values were cropped for plotting and visualization purposes. Raw counts exceed 1200  
560 thus the values are also provided as log transformed (Figure 8). Peak frequency increased  
561 after ca. 400 cal yr BP to ca. 4 fire episodes (periods of increased burning) per 1000 yr  
562 towards present. There was a decrease in grass charcoal indicating increased woody  
563 biomass burned. The increased charcoal influx coupled with low FRI and more woody  
564 charcoal was interpreted as fire episodes that infrequently penetrated the fire sensitive  
565 palm stand and burned the *M. flexuosa* woody biomass. The charcoal, phytolith, and  
566 isotope data collectively suggest that the vegetation surrounding the palm swamp was fire  
567 dependent and fire adapted while the vegetation within the palm swamp was fire  
568 sensitive.

569

570

## 571 **4 Discussion**

572

### 573 *4.1 First Order Control: Edaphic Constraints*

574 Modern vegetation distribution of *cerrado* savannas are largely related to edaphic  
575 factors (Killeen 1998a, Colgan et al. 2012). Since the Lateglacial, the vegetation, soil  
576 geochemistry and fire history indicate edaphic constraints were the first order of control  
577 on vegetation on Huanchaca Mesetta. Despite significant climate variability since the  
578 Lateglacial (Baker et al. 2001, Cruz et al. 2005), the open savanna surrounding the basin  
579 was continuously dominated by fire adapted C<sub>4</sub> grasses. Within the basin, soil was  
580 sufficiently thick to support more complex vegetation communities that exhibited greater  
581 response to climate variability through time. On the highly weathered quartzite plateau  
582 however, vegetation was limited to drought and fire tolerant C<sub>4</sub> grasses as indicated by  
583 the continued presence of C<sub>4</sub> Panicoideae grass phytoliths that co-varied with the  $\delta^{13}\text{C}$   
584 values.

585 The first hypothesis, that edaphic conditions are the dominant control of vegetation  
586 on the plateau, was supported. Irrespective of changes in temperature, precipitation, and  
587 fire activity, savanna vegetation has been present on the mesetta for the past 14,500  
588 years. Edaphic conditions on the open rocky plateau have limited species composition to  
589 C<sub>4</sub> drought adapted grasses. Arboreal and palm vegetation was limited to the topographic  
590 depressions present on the plateau where soil was sufficiently deep to support more  
591 complex vegetation communities.

592

### 593 *4.2 Second Order Control: Climatological Drivers*

594

#### 595 *4.2.1 Lateglacial Surazo Winds and Mauritia flexuosa*

596 Non-analogue Lateglacial vegetation communities are documented from low  
597 elevation sites including Laguna Chaplin (14° 28'S, 61° 04'W approximately 40 km west)  
598 and Laguna Bella Vista (13°, 37'S, 61°, 33W, 140 km northwest). The absence of

599 *Anadenanthera*, a key indicator in present-day deciduous and semi-deciduous dry forests  
600 was interpreted as reduced precipitation (e.g. longer and/or more severe dry season),  
601 increased aridity and lowered atmospheric CO<sub>2</sub> concentrations. These conditions favored  
602 C<sub>4</sub> grasses, sedges and drought adapted savanna and dry forest arboreal species  
603 (Burbridge et al. 2004). Similarly, the non-analogue Lateglacial vegetation community at  
604 Huanchaca Mesetta is notable for the absence of *M. flexuosa*. *M. flexuosa* can tolerate a  
605 broad precipitation gradient ranging from 1500 mm to 3500 mm annually in areas with  
606 annual temperature averages above 21 °C, roughly coinciding with the 1000 m a.s.l.  
607 contour line (Rull and Montoya 2014). *M. f* is dependent on local hydrology including  
608 water table depth and flooded conditions (Kahn 1987). The presence of *M. flexuosa* in the  
609 lowland records at Laguna Chaplin and Laguna Bella Vista (ca. 200 m a.s.l.) during the  
610 Lateglacial (Burbridge et al. 2004), indicate conditions were sufficiently warm and with a  
611 locally wet habitat below the mesetta to support the palms despite an estimated 20%  
612 decrease in precipitation (Mayle et al. 2004, Punyasena 2008). Temperature was thus,  
613 likely a limiting factor for the establishment of *M. flexuosa* on the mesetta. However,  
614 temperature reconstructions of Lateglacial conditions from Laguna La Gaiba, (ca. 500 km  
615 SE of Huanchaca Mesetta), indicate temperatures reached modern conditions (ca. 25 to  
616 26.5 °C) around 19,500 cal yr BP and have remained relatively stable to present (Whitney  
617 et al. 2011). However, previous studies have suggested the increased frequency of  
618 *surazos* winds (Bush and Silman 2004). An ice cap located on the Patagonian Andes  
619 generated an anomalously high pressure center in northwestern Patagonia resulting in  
620 increased *surazo* cold fronts blowing cold, dry, southerly winds northward penetrating  
621 the NKMNP region (Iriondo and Garcia 1993, Latrubesse and Ramonell 1994). The  
622 *surazos* may have been no more intense than those of present, but likely occurred more  
623 often and lasted more of the year (Bush and Silman 2004). Increased frequency of  
624 *surazos* would have had little effect on the absolute temperature minima but the mean  
625 monthly and annual temperature minima may have been ca. 5 °C lower (Bush & Silman,  
626 2004). Based on a lapse rate of 6.4 °C/km (Glickman 2000), the 400 m difference  
627 between the lowland sites (Laguna Chaplin and Laguna Bella Vista, ca. 250 m a.s.l.) and  
628 Huanchaca Mesetta (ca. 650-800 m a.s.l.) could have resulted in up to ca. 2.6 °C  
629 difference in average annual temperatures. Despite near modern annual temperatures  
630 ca.19,500 cal yr BP, the elevational lapse rate coupled with lower mean monthly and  
631 annual temperature minima accompanying more frequent *surazos*, likely resulted in  
632 climatic conditions below the thermal optimum of 21 °C for *M. flexuosa* (Rull and  
633 Montoya 2014). Thus, during the Lateglacial, increased frequency of *surazos* likely  
634 resulted in increased biological stress on the vegetation community at Huanchaca Mesetta  
635 resulting in vegetation dominated by trees and grasses opposed to *M. flexuosa*

636

#### 637 4.2.2 Holocene Precipitation and Fuel Moisture and Fuel Availability

638 During the middle Holocene the presence of dry forest taxa and increased charcoal  
639 influx at Laguna Chaplin and Laguna Bella Vista indicate a combination of seasonally  
640 flooded savannas and semi-deciduous dry forests (Mayle et al. 2004). At Laguna Orícore  
641 (13°20'44.02'S, 63°31'31.86"W, 335 km NW), peaks in drought tolerant arboreal taxa,  
642 coupled with maximum charcoal concentrations indicate drier and regionally more open  
643 vegetation (Carson et al. 2014). Laguna Granja (13°15'44" S, 63°, 42' 37" W) 350 km  
644 NW was also characterized by open savanna vegetation. These data suggest lower mean

645 annual precipitation (<150 cm) and a longer dry season (>5 months with <100 cm) during  
646 the middle Holocene (Mayle et al. 2000, Burbridge et al. 2004). Additionally, water  
647 levels at Lake Titicaca were ca. 100 m below present (Figure 8) attributed to precipitation  
648 levels ca. 40% below present (Cross et al. 2000, Baker et al. 2001, D'Agostino et al.  
649 2002).

650 The discrepancy in increased fire activity in the lowlands sites and decreased fire  
651 activity on the mesetta is attributed to fuel connectivity. In the lowland sites of Laguna  
652 Bella Vista, Laguna Chapin, and Laguna Orícore, dry forest-savanna vegetation provided  
653 sufficient fuel and increased fire activity during the middle Holocene. At Huanchaca  
654 Mesetta decreased available moisture limited vegetation growth and fuel availability,  
655 particularly in the edaphically constrained rocky mesetta surrounding the basin. The lack  
656 of fine C<sub>4</sub> grass connective fuels resulted in decreased burning on the mesetta.

657 In the late Holocene (3750 cal yr BP to present) the pollen assemblages of Laguna  
658 Bella Vista, Laguna Chaplin and Laguna Orícore, indicate an expansion of humid  
659 evergreen closed-canopy rainforest vegetation coupled with significant decreases in  
660 charcoal concentrations (Burbridge et al., 2004; Burn et al., 2010; Carson et al., 2014).  
661 Additionally, Lake Titicaca reach modern water levels during this time (Rowe et al.  
662 2003) indicating wetter regional conditions with less severe dry seasons. The rainforest–  
663 savanna ecotone is currently at its most southerly extent over at least the last 50,000 years  
664 (Mayle et al. 2000; Mayle and Whitney, 2012; Burbridge et al. et al., 2004). The  
665 progressive succession through the Holocene in the lowlands of NKMNP from  
666 savanna/semi-deciduous forest to semi-deciduous/evergreen forest to evergreen rainforest  
667 is part of a long-term uni-directional trend of climate-driven rainforest expansion  
668 associated with the regional increase in precipitation associated with a stronger SASM  
669 (Mayle et al. 2004). The basin wide increase in mean annual precipitation and reduction  
670 in the length/severity of the dry season is attributed to increasing summer insolation at  
671 10-15°S driven by the Milankovitch precessional forcing (Mayle and Whitney 2012). The  
672 wet conditions of the late Holocene created ideal waterlogged conditions for the  
673 establishment of the *M. flexuosa* palm swamp in the drainage basin.

674 The asynchrony of charcoal records between the low elevation sites and Huanchaca  
675 Mesetta is attributed to fuel flammability. Increased precipitation led to different effects  
676 on fire frequency, with decreases in the lowlands and increases on Huanchaca Mesetta.  
677 Increased precipitation in the low elevation closed canopy rainforests decreased fuel  
678 flammability along with fire activity. Whereas increased precipitation resulted in the  
679 build up of fire-adapted C<sub>4</sub> grasses on the surrounding plateau. Lightning-caused fire is  
680 common in *cerrão* savannas today and highest in more open savanna ecosystems, such  
681 as the Huanchaca Mesetta (Ramos-Neto and Pivello 2000). Increased precipitation would  
682 have been accompanied by increased incidence of lightning-caused fire, fueled by the  
683 abundance of fire adapted grass fuels in the surrounding watershed.

684 The second hypothesis, that climate was the dominant control on savanna vegetation  
685 structure and floristic composition was supported by the vegetation and fire data. Since  
686 the Lateglacial, climate change has coincided with both the vegetation composition and  
687 fire regimes on the plateau. The asynchrony in response to regional climate forcing at  
688 Huanchaca Mesetta and the low elevation sites emphasize the need to obtain more  
689 paleorecords across an elevational gradient to determine the effects of climate variability  
690 across heterogeneous ecosystems.

691

692 4.3 Human versus Natural Drivers on the Evolution of *Mauritia flexuosa*

693 The development of *M. flexuosa* swamps and increases in charcoal influx have been  
694 seen in numerous paleoecological records from savanna ecosystems in Colombia  
695 (Behling and Hooghiemstra 1998, 1999, Berrio et al. 2002a, 2002b), Venezuela (Rull  
696 1999, 2009, Montoya et al. 2011b, Rull and Montoya 2014) and Brazil (Da Silva  
697 Meneses et al. 2013). Previously two hypotheses have been proposed to account for the  
698 late Holocene development of these *M. flexuosa* palm swamps. The first hypothesis  
699 suggests that the increase in *M. flexuosa* and charcoal influx is attributed to increased  
700 precipitation and wet season lightning fires driven by strengthened SASM activity (Kahn  
701 and de Castro 1985, Kahn 1987, Kahn and de Granville 1992). The second hypothesis  
702 suggest that the simultaneous rise in *M. flexuosa* and charcoal was linked to intentional  
703 planting or semi-domestication of *M. flexuosa* for human use (Behling and Hooghiemstra  
704 1998, 1999, Montoya et al. 2011a, Rull and Montoya 2014). Currently there is  
705 insufficient archaeological evidence from any of these savanna sites to support a robust  
706 anthropogenic signal (Rull and Montoya 2014). Previous paleoecological studies in the  
707 lowlands demonstrate humans were the dominant driver of local-scale forest-savanna  
708 ecotonal change in those areas (e.g. Bolivian *Llanos de Moxos*) dominated by complex  
709 earth-moving pre-Columbian cultures (Whitney et al. 2014, Carson et al. 2014). These  
710 studies suggest that even in areas with extensive geometric earthworks, inhabitants likely  
711 exploited naturally open savanna landscapes that they maintained around their settlement,  
712 rather than practicing labor-intensive deforestation of dense rainforest (Carson et al.  
713 2014). Evidence for human occupation of the lowlands has been found with ceramics  
714 from soil pits in an interfluvial ca. 25 km northwest of Laguna Chaplin and abundant  
715 ceramics and charcoal dating to ca. 470 cal yr BP recovered from anthosols (terra preta)  
716 throughout La Chonta ca. 150 km west of NKMNP (Burbridge et al. 2004).  
717 Implementing a new methodology to concentrate and isolate cultigen pollen (Whitney et  
718 al. 2012), the re-analysis of pollen data from Laguna Bella Vista and Laguna Chaplin  
719 revealed *Zea mays* pollen was present around 1000 to 400 cal yr BP, approximately 2000  
720 years after the initial increase in *M. flexuosa* at these sites (B. Whitney personal  
721 communication, 2014). Although humans were present in NKMNP, there is no evidence  
722 that they drove regionally significant ecotonal changes in forest-savanna boundaries. The  
723 patterns of forest-savanna shifts exhibited at these sites are consistent with climate  
724 forcing (Burbridge et al. 2004). The absence of archaeological data on Huanchaca  
725 Mesetta dominated by nutrient poor, rocky soil, that would have been infertile for the  
726 practice of agriculture coupled with the limited access to the mesetta would have made  
727 human habitation unlikely. Although the *M. flexuosa* swamps may have been used for  
728 hunting and gathering purposes, these data do not suggest humans were the driving  
729 mechanism behind the initial establishment or proliferation of *M. flexuosa* in the  
730 interfluvial depressions of the Mesetta.

731 The comparison of the Huanchaca Mesetta record to previous studies coupled with  
732 the absence of archaeological remains on the mesetta support the third hypothesis, that  
733 expansion of *M. flexuosa* at this site was largely controlled by natural drivers (edaphic,  
734 climate, lightning caused fires) opposed to anthropogenic drivers. In contrast to the  
735 conclusions from other studies, this record provides no evidence for an  
736 anthropogenically-driven fire regime, deforestation, soil erosion, or cultivation on the



737 mesetta. These data suggest that natural drivers control the continued presence of savanna  
738 vegetation and fire activity on the Huanchaca Mesetta for the past 14,500 years.

### 739 *5.0 Implications for Savanna Ecology and Conservation*

740 The presence of savanna vegetation for the past 14,500 years at Huanchaca Mesetta  
741 has significant implications for understanding modern savanna ecology and for the  
742 implementation of conservation strategies in the 21<sup>st</sup> century. Previous research on the  
743 evolution and development of savanna ecosystems has attributed much of the  
744 development of savannas to anthropogenic origins driven by the intentional use of fire  
745 (Behling and Hooghiemstra 1999, Ramos-Neto and Pivello 2000, Behling 2002, Berrio et  
746 al. 2002a, Arroyo-Kalin 2012, Rull and Montoya 2014) (Behling and Hooghiemstra  
747 1998, 1999, Ramos-Neto and Pivello 2000, Behling 2002, Berrio et al. 2002a, Arroyo-  
748 Kalin 2012, Rull and Montoya 2014). The results from this study demonstrate that the  
749 continued presence of the savanna ecosystem at Huanchaca Mesetta is attributable to  
750 edaphic and climatic controls. The presence of fire in this system for the past 14,500  
751 years indicates that naturally occurring, lightning-caused fire is an integral part of the  
752 ecology of the savanna ecosystem. Despite changes in floristic composition and tree  
753 density within the drainage basin, the savanna ecosystem has been resilient to major  
754 climatic changes in both temperature and precipitation since the Lateglacial period. These  
755 data suggest that savanna ecosystems will continue to be resilient to future climate  
756 change associated with global warming. The long history of ecosystem stability in the  
757 face of dramatic climate variability attests to the fact that the Huanchaca Mesetta savanna  
758 is one of the most floristically diverse savannas anywhere in the Neotropics (Da Silva  
759 Meneses and Bates 2002). The continued protection of the Huanchaca Mesetta savanna  
760 as a UNESCO world heritage site, coupled with the savannas natural resilience to  
761 climatic change exhibited over at least the past 14,500 years, indicates that despite  
762 significant global warming projected for the 21<sup>st</sup> century (IPCC 2014), the future is  
763 optimistic for the conservation and preservation of biological diversity in the Huanchaca  
764 Mesetta savanna ecosystem.

765

766

### 767 **Acknowledgements**

768 Funding to Y.M. was provided by Global Change and Sustainability Center, the Graduate  
769 Research Fellowship, the Don Currey Graduate Research Fellowship, and the PAGES  
770 Graduate Research Fellowship. We thank Mary McIntyre and Daniel Harris for their help  
771 in sample preparation and analysis. Jennifer Watling and the Archaeobotany Lab at the  
772 University of Exeter assisted in phytolith training. Lee Grismer provided support for this  
773 research. The University of Leicester provided funding to FM. We thank Dr. Tim Killeen  
774 and the Museo de Historia Natural ‘Noel Kempff Mercado’, Santa Cruz, Bolivia for  
775 providing logistical support, and in particular Rene Guillen and local guides from the  
776 village of Florida (e.g. Juan Surubi) for assistance with coring the site.

777

778

779

780 **References**

- 781 Abreu, M. F., J. R. R. Pinto, L. Maracahipes, L. Gomes, E. A. de Oliveira, B. S.  
782 Marimon, M. Junior, B. Hur, J. de Farias, and E. Lenza. 2012. Influence of edaphic  
783 variables on the floristic composition and structure of the tree-shrub vegetation in  
784 typical and rocky outcrop cerrado areas in Serra Negra, Goiás State, Brazil.  
785 *Brazilian Journal of Botany* 35:259–272.
- 786 Arroyo-Kalin, M. 2012. Slash-burn-and-churn: Landscape history and crop cultivation in  
787 pre-Columbian Amazonia. *Quaternary International* 249:4–18.
- 788 Baker, P. A., G. O. Seltzer, S. C. Fritz, R. B. Dunbar, M. J. Grove, P. M. Tapia, S. L.  
789 Cross, H. D. Rowe, and J. P. Broda. 2001. The history of South American tropical  
790 precipitation for the past 25,000 years. *Science (New York, N.Y.)* 291:640–3.
- 791 Behling, H. 2002. South and southeast Brazilian grasslands during Late Quaternary  
792 times: A synthesis. *Palaeogeography, Palaeoclimatology, Palaeoecology* 177:19–27.
- 793 Behling, H., and H. Hooghiemstra. 1998. Late Quaternary palaeoecology and  
794 palaeoclimatology from pollen records of the savannas of the Llanos Orientales in  
795 Colombia. *Palaeogeography, Palaeoclimatology, Palaeoecology* 139:251–267.
- 796 Behling, H., and H. Hooghiemstra. 1999. Environmental history of the Colombian  
797 savannas of the Llanos Orientales since the Last Glacial Maximum from lake  
798 records El Pinal and Carimagua. *Journal of Paleolimnology* 21:461–476.
- 799 Bennett, K. D. 1996. Determination of the number of zones in a biostratigraphical  
800 sequence. *New Phytologist* 132:155–170.
- 801 Berrio, J. C., H. Hooghiemstra, H. Behling, P. Botero, and K. Van der Borg. 2002a. Late-  
802 Quaternary savanna history of the Colombian Llanos Orientales from Lagunas  
803 Chenevo and Mozambique: A transect synthesis. *The Holocene* 12:35–48.
- 804 Berrio, J. C., H. Hooghiemstra, R. Marchant, and O. Rangel. 2002b. Late-glacial and  
805 Holocene history of the dry forest area in the south Colombian Cauca Valley.  
806 *Journal of Quaternary Science* 17:667–682.
- 807 Bertoli de Pomar, H. 1971. Ensayo de clasificacion morfologica de los silicofitolitos.  
808 *Ameghiniana* 3:317–328.
- 809 Blaauw, M. 2010. Methods and code for “classical” age-modelling of radiocarbon  
810 sequences. *Quaternary Geochronology* 5:512–518.
- 811 Brown, K. J., and M. J. Power. 2013. Charred particle analyses. Pages 716–729 *The*  
812 *Encyclopedia of Quaternary Science*. Second edition. Elsevier, Amsterdam, The  
813 Netherlands.

- 814 Burbridge, R. E., F. E. Mayle, and T. J. Killeen. 2004. Fifty-thousand-year vegetation and  
815 climate history of Noel Kempff Mercado National Park, Bolivian Amazon.  
816 *Quaternary Research* 61:215–230.
- 817 Burn, M. J., F. E. Mayle, and T. J. Killeen. 2010. Pollen-based differentiation of  
818 Amazonian rainforest communities and implications for lowland palaeoecology in  
819 tropical South America. *Palaeogeography, Palaeoclimatology, Palaeoecology*  
820 295:1–18.
- 821 Bush, M. B., and M. R. Silman. 2004. Observations on Late Pleistocene cooling and  
822 precipitation in the lowland Neotropics. *Journal of Quaternary Science* 19:677–684.
- 823 Carson, J. F., B. S. Whitney, F. E. Mayle, J. Iriarte, H. Prümers, J. D. Soto, and J.  
824 Watling. 2014. Environmental impact of geometric earthwork construction in pre-  
825 Columbian Amazonia. *Proceedings of the National Academy of Sciences of the*  
826 *United States of America* 111:1–6.
- 827 Codron, J., D. Codron, J. A. Lee-Thorp, M. Sponheimer, W. J. Bond, D. de Ruiter, and R.  
828 Grant. 2005. Taxonomic, anatomical, and spatio-temporal variations in the stable  
829 carbon and nitrogen isotopic compositions of plants from an African savanna.  
830 *Journal of Archaeological Science* 32:1757–1772.
- 831 Colgan, M. S., G. P. Asner, S. R. Levick, R. E. Martin, and O. A. Chadwick. 2012. Topo-  
832 edaphic controls over woody plant biomass in South African savannas.  
833 *Biogeosciences* 9:957–987.
- 834 Cross, S. L., P. A. Baker, G. O. Seltzer, S. C. Fritz, and R. B. Dunbar. 2000. A new  
835 estimate of the Holocene lowstand level of Lake Titicaca, central Andes, and  
836 implications for tropical palaeohydrology. *The Holocene* 10:21–32.
- 837 Cruz, F. W., S. J. Burns, and I. Karmann. 2005. Insolation-driven changes in atmospheric  
838 circulation over the past 116,000 years in subtropical Brazil. *Nature* 434:63–66.
- 839 D’Agostino, K., G. Seltzer, P. Baker, S. Fritz, and R. Dunbar. 2002. Late-Quaternary  
840 lowstands of Lake Titicaca: Evidence from high-resolution seismic data.  
841 *Palaeogeography, Palaeoclimatology, Palaeoecology* 179:97–111.
- 842 Dean Jr, W. E. 1974. Determination of carbonate and organic matter in calcareous  
843 sediments and sedimentary rocks by loss on ignition: comparison with other  
844 methods. *Journal of Sedimentary Research* 44.
- 845 Fidelis, A. T., M. D. Delgado Cartay, C. C. Blanco, S. C. Muller, V. de P. Pillar, and J. S.  
846 Pfadenhauer. 2010. Fire intensity and severity in Brazilian Campos grasslands.  
847 *Interciencia: revista de ciencia y tecnologia de america* 35:739–745.

- 848 Fredlund, G. G., and L. T. Tieszen. 1994. Modern phytolith assemblages from the North  
849 American Great Plains. *Journal of Biogeography* 21:321–335.
- 850 Furley, P. A., and J. A. Ratter. 1988. Soil resources and plant communities of the central  
851 Brazilian cerrado and their development. *Journal of Biogeography* 15:97–108.
- 852 Gedye, S. J., R. T. Jones, W. Tinner, B. Ammann, and F. Oldfield. 2000. The use of  
853 mineral magnetism in the reconstruction of fire history: A case study from Lago di  
854 Origlio, Swiss Alps. *Palaeogeography, Palaeoclimatology, Palaeoecology* 164:101–  
855 110.
- 856 Glickman, T. S. 2000. *Glossary of meteorology*. 2nd edition. American Meteorological  
857 Society, Boston, MA.
- 858 Grimm, E. C. 1987. CONISS: A Fortran 77 program for stratigraphically constrained  
859 cluster analysis by the method of the incremental sum of squares. *Computers and*  
860 *Geosciences* 13:13–35.
- 861 Hanagarth, W. 1993. Acerca de la geocología de las sabanas del Beni en el noreste de  
862 Bolivia. Instituto de Ecología, La Paz, Bolivia.
- 863 Hardesty, J., R. Myers, and W. Fulks. 2005. Fire, ecosystems, and people: A preliminary  
864 assessment of fire as a global conservation issue. *The George Wright Forum* 22:78–  
865 87.
- 866 Haridasan, M. 2000. Nutrição mineral de plantas nativas do cerrado. *Revista Brasileira de*  
867 *Fisiologia Vegetal* 12:54–64.
- 868 Hartley, W. 1958a. Studies on the origin, evolution, and distribution of the Gramineae. II.  
869 The Tribe Paniceae. *Australian Journal of Botany* 6:343–357.
- 870 Hartley, W. 1958b. Studies on the origin, evolution, and distribution of the Gramineae. I.  
871 The tribe Andropogoneae. *Australian Journal of Botany* 6:115–128.
- 872 Hartley, W. 1961. Studies on the origin, evolution, and distribution of the Gramineae. IV.  
873 The genus *Poa* L. *Australian Journal of Botany Ecology* 9:152–161.
- 874 Hartley, W. 1973. Studies on the origin, evolution, and distribution of the Gramineae. V.  
875 The subfamily Festucoideae. *Australian Journal of Botany* 21:201–234.
- 876 Hartley, W., and C. Slater. 1960. Studies on the origin, evolution, and distribution of the  
877 Gramineae. III. The tribes of the subfamily Eragrostoideae. *Australian Journal of*  
878 *Botany* 8:256–276.

- 879 Higuera, P. E., L. B. Brubaker, P. M. Anderson, S. H. Feng, and A. Brown, Thomas.  
880 2009. Vegetation mediated the impacts of postglacial climate change on fire regimes  
881 in the south-central Brooks Range, Alaska. *Ecological Monographs* 79:201–219.
- 882 Higuera, P., M. Peters, L. Brubaker, and D. Gavin. 2007. Understanding the origin and  
883 analysis of sediment-charcoal records with a simulation model. *Quaternary Science*  
884 *Reviews* 26:1790–1809.
- 885 Huber, O. 1995a. Geographical and physical features. Pages 1–62 in P. E. Berry, B. K.  
886 Holst, and K. Yatskievych, editors. *Flora of the Venezuelan Guayana*. Missouri  
887 Botanical Garden, St. Louis, MO.
- 888 Huber, O. 1995b. Vegetation. Pages 97–160 in P. E. Berry, B. K. Holst, and K.  
889 Yatskievych, editors. *Flora of the Venezuelan Guayana*. Missouri Botanical Garden,  
890 St. Louis, MO.
- 891 IPCC, 2014. 2014. *Climate Change 2014: Impacts, adaptation, and vulnerability. Part A:*  
892 *Global and sectoral aspects. IPCC 2014*. Cambridge University Press, Cambridge,  
893 England.
- 894 Iriarte, J. 2003. Assessing the feasibility of identifying maize through the analysis of  
895 cross-shaped size and three-dimensional morphology of phytoliths in the grasslands  
896 of southeastern South America. *Journal of Archaeological Science* 30:1085–1094.
- 897 Iriarte, J. 2006. Vegetation and climate change since 14,810 14C yr B.P. in southeastern  
898 Uruguay and implications for the rise of early Formative societies. *Quaternary*  
899 *Research* 65:20–32.
- 900 Iriarte, J., and E. A. Paz. 2009. Phytolith analysis of selected native plants and modern  
901 soils from southeastern Uruguay and its implications for paleoenvironmental and  
902 archeological reconstruction. *Quaternary International* 193:99–123.
- 903 Iriando, M., and N. Garcia. 1993. Climatic variations in the Argentine plains during the  
904 last 18,000 years. *Palaeogeography, palaeoclimatology, palaeoecology* 101:209–  
905 220.
- 906 Jensen, K., E. A. Lynch, R. Calcote, and S. C. Hotchkiss. 2007. Interpretation of charcoal  
907 morphotypes in sediments from Ferry Lake, Wisconsin, USA: Do different plant  
908 fuel sources produce distinctive charcoal morphotypes? *The Holocene* 17:907–915.
- 909 Junior, B. H. M., and M. Haridasan. 2005. Comparação da vegetação arbórea e  
910 características edáficas de um cerradão e um cerrado sensu stricto em áreas  
911 adjacentes sobre solo distrófico no leste de Mato Grosso, Brasil. *Acta Botanica*  
912 *Brasilica* 19:913–926.

- 913 Kahn, F. 1987. The distribution of palms as a function of local topography in Amazonian  
914 terra-firme forests. *Cellular and Molecular Life Sciences* 43:251–259.
- 915 Kahn, F. 1988. Ecology of economically important palms in Peruvian Amazonia.  
916 *Advances in Economic Botany* 6:42–49.
- 917 Kahn, F., and A. de Castro. 1985. The palm community in a forest of central Amazonia,  
918 Brazil. *Biotropica* 1:210–216.
- 919 Kahn, F., and J. J. de Granville. 1992. Palms in forest ecosystems of Amazonia  
920 ecological studies 98. Springer-Verlag, Heidelberg, Germany.
- 921 Killeen, T. J. 1990. The grasses of Chiquitanía, Santa Cruz, Bolivia. *Annals of the*  
922 *Missouri Botanical Garden* 1:125–201.
- 923 Killeen, T. J. 1998a. Geomorphology of the Huanchaca Plateau and surrounding areas.  
924 Pages 43–46 *in* T. J. Killeen and T. S. Schulenberg, editors. A biological assessment  
925 of Parque Nacional Noel Kempff Mercado, Bolivia. Conservation International,  
926 Washington, DC.
- 927 Killeen, T. J. 1998b. Vegetation and flora of Parque Nacional Noel Kempff Mercado.  
928 Pages 61–85 *in* T. J. Killeen and T. S. Schulenberg, editors. A biological assessment  
929 of Parque Nacional Noel Kempff Mercado, Bolivia. Conservation International,  
930 Washington, DC.
- 931 Killeen, T. J., and T. S. Schulenberg. 1998. Vegetation and flora of Noel Kempff  
932 Mercado National Park. A biological assessment of Parque Nacional Noel Kempff  
933 Mercado, Bolivia. RAP working papers 10. Conservation International, Washington,  
934 DC.
- 935 Killeen, T. J., T. M. Siles, T. Grimwood, L. L. Tieszen, M. K. Steininger, C. J. Tucker,  
936 and S. Panfil. 2003. Habitat heterogeneity on a forest-savanna ecotone in Noel  
937 Kempff Mercado National Park (Santa Cruz, Bolivia): Implications for the long-  
938 term conservation of biodiversity in a changing climate. Pages 285–312 *in* G.  
939 Bradshaw and P. Marquet, editors. *How Landscapes Change*. Springer Verlag,  
940 Berlin.
- 941 Latrubesse, E. M., and C. G. Ramonell. 1994. A climatic model for southwestern  
942 Amazonia in last glacial times. *Quaternary international* 21:163–169.
- 943 Latrubesse, E. M., J. C. Stevaux, E. H. Cremon, J.-H. May, S. H. Tatumi, M. a. Hurtado,  
944 M. Bezada, and J. B. Argollo. 2012. Late Quaternary megafans, fans and fluvio-  
945 aeolian interactions in the Bolivian Chaco, Tropical South America.  
946 *Palaeogeography, Palaeoclimatology, Palaeoecology* 356:75–88.

- 947 Litherland, M., and G. Power. 1989. The geologic and geomorphic evolution of Serrania  
948 Huanchaca (Eastern Bolivia): The lost world. *Journal of South American Earth*  
949 *Science* 2:1–17.
- 950 Malamud-Roam, F. P., L. B. Ingram, M. Hughes, and J. L. Florsheim. 2006. Holocene  
951 paleoclimate records from a large California estuarine system and its watershed  
952 region: Linking watershed climate and bay conditions. *Quaternary Science Reviews*  
953 25:1570–1598.
- 954 Malhi, Y., P. Meir, and S. Brown. 2002. Forests, carbon and global climate.  
955 *Philosophical Transactions of the Royal Society of London. Series A: Mathematical,*  
956 *Physical and Engineering Sciences* 360:1567–1591.
- 957 Marlon, J. R., P. J. Bartlein, C. Carcaillet, D. G. Gavin, S. P. Harrison, P. E. Higuera, F.  
958 Joos, M. J. Power, and I. C. Prentice. 2008. Climate and human influences on global  
959 biomass burning over the past two millennia. *Nature Geoscience* 1:697–702.
- 960 Marlon, J. R., P. J. Bartlein, A. Daniiau, S. P. Harrison, S. Y. Maezumi, M. J. Power, W.  
961 Tinner, and B. Vanni re. 2013. Global biomass burning: A synthesis and review of  
962 Holocene paleofire records and their controls. *Quaternary Science Reviews* 65:5–25.
- 963 Mayle, F. E., D. J. Beerling, W. D. Gosling, and M. B. Bush. 2004. Responses of  
964 Amazonian ecosystems to climatic and atmospheric carbon dioxide changes since  
965 the last glacial maximum. *Philosophical transactions of the Royal Society of*  
966 *London. Series B, Biological sciences* 359:499–514.
- 967 Mayle, F. E., R. Burbridge, and T. J. Killeen. 2000. Millennial-scale dynamics of  
968 southern Amazonian rain forests. *Science* 290:2291–2294.
- 969 Mayle, F. E., R. P. Langstroth, R. a Fisher, and P. Meir. 2007. Long-term forest-savannah  
970 dynamics in the Bolivian Amazon: implications for conservation. *Philosophical*  
971 *transactions of the Royal Society of London. Series B, Biological sciences* 362:291–  
972 307.
- 973 Mayle, F. E., and B. S. Whitney. 2012. Long-term perspectives on tropical forest-savanna  
974 dynamics in lowland bolivia from the last ice age until present. Pages 189–207 *in* R.  
975 W. Myster, editor. *Ecotones Between Forest and Grassland*. Springer, London,  
976 England.
- 977 McCormac, F. G., A. G. Hogg, P. G. Blackwell, C. E. Buck, T. F. G. Higham, and P. J.  
978 Reimer. 2004. SHCAL04 southern hemisphere calibration, 0-11.0 cal KYR BP.  
979 *Radiocarbon* 46:1087–1092.
- 980 McLauchlan, K. K., I. Lascu, A. Myrbo, and P. R. Leavitt. 2013. Variable ecosystem  
981 response to climate change during the Holocene in northern Minnesota, USA. *The*  
982 *Geological Society of America Bulletin* 23:1635–1643.

- 983 Miranda, H. S., M. N. Sato, W. N. Neto, and F. S. Aires. 2009. Fires in the Cerrado, the  
 984 Brazilian savanna. Pages 427–450 in M. A. Cochrane, editor. *Tropical Fire Ecology: climate change, land use and ecosystem dynamics*. Springer, Berlin, Germany.  
 985
- 986 Mistry, J. 1998. Fire in the Cerrado (savannas) of Brazil: An ecological review. *Progress*  
 987 *in Physical Geography* 22:425–448.
- 988 Mittermeier, R. A., N. Myers, C. G. Mittermeier, and P. Robles Gil. 1999. Hotspots:  
 989 Earth's biologically richest and most endangered terrestrial ecoregions. CEMEX,  
 990 SA, Agrupación Sierra Madre, Mexico.
- 991 Montes de Oca, I. 1982. *Geografía y recursos naturales de Bolivia*. 3rd Editio. Edobol, La  
 992 Paz, Bolivia.
- 993 Montoya, E., and V. Rull. 2011. Gran Sabana fires (SE Venezuela): a paleoecological  
 994 perspective. *Quaternary Science Reviews* 30:3430–3444.
- 995 Montoya, E., V. Rull, and S. Nogué. 2011a. Early human occupation and land use  
 996 changes near the boundary of the Orinoco and the Amazon basins (SE Venezuela):  
 997 Palynological evidence from El Paují record. *Palaeogeography, Palaeoclimatology,*  
 998 *Palaeoecology* 310:413–426.
- 999 Montoya, E., V. Rull, N. D. Stansell, M. B. Abbott, S. Nogué, B. W. Bird, and W. A.  
 1000 Díaz. 2011b. Forest – savanna – morichal dynamics in relation to fire and human  
 1001 occupation in the southern Gran Sabana ( SE Venezuela ) during the last millennia.  
 1002 *Quaternary Research* 76:335–344.
- 1003 Mueller, J. R., C. J. Long, J. J. Williams, A. Nurse, and K. K. McLauchlan. 2014. The  
 1004 relative controls on forest fires and fuel source fluctuations in the Holocene  
 1005 deciduous forests of southern Wisconsin, USA. *Journal of Quaternary Science*  
 1006 29:561–569.
- 1007 Myers, N., R. A. Mittermeier, C. G. Mittermeier, G. A. Da Fonseca, and J. Kent. 2000.  
 1008 Biodiversity hotspots for conservation priorities. *Nature* 403:853–8.
- 1009 Nowaczyk, N. R. 2001. Logging of magnetic susceptibility. Pages 155–170 *Tracking*  
 1010 *environmental change using lake sediments*. Springer Netherlands, Potsdam,  
 1011 Germany.
- 1012 Perdue, E. M., and J.-F. Koprivnjak. 2007. Using the C/N ratio to estimate terrigenous  
 1013 inputs of organic matter to aquatic environments. *Estuarine, Coastal and Shelf*  
 1014 *Science* 73:65–72.
- 1015 Pereira, J. M. C. 2003. Remote sensing of burned areas in tropical savannas. *International*  
 1016 *Journal of Wildland Fire* 12:259–270.



- 1017 Piperno, D. R. 1997. Phytoliths and microscopic charcoal from leg 155: A vegetational  
1018 and fire history of the Amazon Basin during the last 75 Ky., Pages 411–418  
1019 Proceedings of the Ocean Drilling Program. Scientific Results.
- 1020 Piperno, D. R. 2005. Phytoliths: A comprehensive guide for archaeologists and  
1021 paleoecologists. Altamira Press, Oxford, England.
- 1022 Piperno, D. R., and D. M. Pearsall. 1998. The silica bodies of tropical American grasses:  
1023 Morphology, taxonomy, and implication from grass systematics and fossil phytolith  
1024 identification. Smithsonian Institution Press, Washington, DC.
- 1025 Pivello, V. R. 2011. The use of fire in the Cerrado and Amazonian rainforests of Brazil:  
1026 Past and present. *Fire ecology* 7:24–39.
- 1027 Punyasena, S. W. 2008. Estimating neotropical palaeotemperature and  
1028 palaeoprecipitation using plant family climatic optima. *Palaeogeography,*  
1029 *Palaeoclimatology, Palaeoecology* 265:226–237.
- 1030 Ramos-Neto, M. B., and V. R. Pivello. 2000. Lightning fires in a Brazilian savanna  
1031 National Park: Rethinking management strategies. *Environmental Management*  
1032 26:675–684.
- 1033 Reimer, P. J., E. Bard, A. Bayliss, J. W. Beck, P. G. Blackwell, C. Bronk Ramsey, C. E.  
1034 Buck, H. Cheng, R. L. Edwards, and M. Friedrich. 2013. IntCal13 and Marine13  
1035 radiocarbon age calibration curves 0-50,000 years cal BP.
- 1036 Reynolds, R., J. Belnap, M. Reheis, P. Lamothe, and F. Luiszer. 2001. Aeolian dust in  
1037 Colorado Plateau soils: Nutrient inputs and recent change in source. *Proceedings of*  
1038 *the National Academy of Sciences* 98:7123–7127.
- 1039 Ribeiro, J. F., and B. M. T. Walter. 2008. As principais fitofisionomias do Bioma  
1040 Cerrado. Pages 151–212 *Cerrado: Ecologia e flora*. Embrapa-CPAC, Planaltina,  
1041 Brazil.
- 1042 Robinson, D. 1991. *Roots and resources fluxes in plant and communities*. Blackwell  
1043 Scientific Publications, Oxford, England.
- 1044 Roche, M.A., Rocha, N. 1985. Precipitaciones anuales. Programa climatológico e  
1045 hidrológico de la Cuenca Amazónica Boliviana (PHICAB). Servicio Nacional de  
1046 Meteorología e Hidrología (SENAHMHI), La Paz, Bolivia.
- 1047 Rowe, H. D., T. P. Guilderson, R. B. Dunbar, J. R. Southon, G. O. Seltzer, D. A.  
1048 Mucciarone, S. C. Fritz, and P. A. Baker. 2003. Late Quaternary lake-level changes  
1049 constrained by radiocarbon and stable isotope studies on sediment cores from Lake  
1050 Titicaca, South America. *Global and Planetary Change* 38:273–290.

- 1051 Rull, V. 1999. A palynological record of a secondary succession after fire in the Gran  
1052 Sabana, Venezuela. *Journal of Quaternary Science* 14:137–152.
- 1053 Rull, V. 2009. On the use of paleoecological evidence to assess the role of humans in the  
1054 origin of the Gran Sabana (Venezuela). *Human Ecology* 37:783–785.
- 1055 Rull, V., and E. Montoya. 2014. *Mauritia flexuosa* palm swamp communities: Natural or  
1056 human-made? A palynological study of the Gran Sabana region (northern South  
1057 America) within a neotropical context. *Quaternary Science Reviews* 99:17–33.
- 1058 Russell-Smith, J., D. Lucas, M. Gapindi, N. Kapirigi, G. Namingum, P. Giuliani, and G.  
1059 Chaloupka. 1997. Aboriginal resource utilization and fire management practice in  
1060 western Arnhem land, monsoonal northern Australia: Notes for prehistory, lessons  
1061 for the future. *Human Ecology* 25:159–195.
- 1062 Seitzinger, S., J. A. Harrison, J. K. Böhlke, A. F. Bouwman, R. Lowrance, B. Peterson,  
1063 C. Tobias, and G. Van Drecht. 2006. Denitrification across landscapes and  
1064 waterscapes: A synthesis. *Ecological Applications* 16:2064–2090.
- 1065 Sendulsky, T., and L. G. Labouriau. 1966. *Corpos siliceos de Gramineas dos Cerrados-I.*  
1066 *Anais da Academia Brasileira de Ciencias* 38:159–185.
- 1067 Da Silva Meneses, J. M. C., and J. M. Bates. 2002. Biogeographic patterns and  
1068 conservation in the South American cerrado: A tropical savanna hotspot. *BioScience*  
1069 52:225–234.
- 1070 Da Silva Meneses, M. E. N., M. L. Da Costa, and H. Behling. 2013. Late Holocene  
1071 vegetation and fire dynamics from a savanna-forest ecotone in Roraima state,  
1072 northern Brazilian Amazon. *Journal of South American Earth Sciences* 42:17–26.
- 1073 Söndahl, M. R.-I., and L. G. Labouriau. 1970. *Corpos silicosos de gramíneas dos*  
1074 *Cerrados. IV. Pesquisa Agropecuária Brasileira* 5:183–207.
- 1075 Teixeira da Silva, S., and L. G. Labouriau. 1970. *Corpos siliceos de gramineas dos*  
1076 *Cerrados-III. Pesquisas Agropecuarias Brasileiras* 5:167–182.
- 1077 Tweiten, M. A., S. C. Hotchkiss, R. K. Booth, R. R. Calcote, and E. A. Lynch. 2009. The  
1078 response of a jack pine forest to late-Holocene climate variability in northwestern  
1079 Wisconsin. *The Holocene* 19:1049–1061.
- 1080 Twiss, P. C., E. Suess, and R. M. Smith. 1969. Morphological classification of grass  
1081 phytoliths. *Proceedings of Soil Science of America* 33:109–115.
- 1082 Vuille, M., S. J. Burns, B. L. Taylor, F. W. Cruz, B. W. Bird, M. B. Abbott, L. C.  
1083 Kanner, H. Cheng, and V. F. Novello. 2012. A review of the South American

- 1084 monsoon history as recorded in stable isotopic proxies over the past two millennia.  
1085 *Climate of the Past* 8:1309–1321.
- 1086 Van der Werf, G. R., J. T. Randerson, L. Giglio, G. J. Collatz, M. Mu, P. S. Kasibhatla,  
1087 D. C. Morton, R. S. DeFries, Y. Jin, and T. T. Van Leeuwen. 2010. Global fire  
1088 emissions and the contribution of deforestation, savanna, forest, agricultural, and  
1089 peat fires (1997–2009). *Atmospheric Chemistry and Physics* 10:11707–11735.
- 1090 Whitlock, C., and C. Larsen. 2001. Charcoal as a fire proxy. Pages 75–97 *Tracking*  
1091 *environmental change using lake sediments*. Kluwer Academic Publishers,  
1092 Dordrecht, The Netherlands.
- 1093 Whitney, B. S., R. Dickau, F. E. Mayle, J. H. Walker, J. D. Soto, and J. Iriarte. 2014. Pre-  
1094 Columbian raised-field agriculture and land use in the Bolivian Amazon. *The*  
1095 *Holocene* 24:231–241.
- 1096 Whitney, B. S., F. E. Mayle, S. W. Punyasena, K. A. Fitzpatrick, M. J. Burn, R. Guillen,  
1097 E. Chavez, D. Mann, R. T. Pennington, and S. E. Metcalfe. 2011. A 45kyr  
1098 palaeoclimate record from the lowland interior of tropical South America.  
1099 *Palaeogeography, Palaeoclimatology, Palaeoecology* 307:177–192.
- 1100 Whitney, B. S., E. a. Rushton, J. F. Carson, J. Iriarte, and F. E. Mayle. 2012. An  
1101 improved methodology for the recovery of *Zea* mays and other large crop pollen,  
1102 with implications for environmental archaeology in the Neotropics. *The Holocene*  
1103 22:1087–1096.
- 1104 Willis, K. J., M. B. Araújo, K. D. Bennett, B. Figueroa-Rangel, C. a Froyd, and N.  
1105 Myers. 2007. How can a knowledge of the past help to conserve the future?  
1106 *Biodiversity conservation and the relevance of long-term ecological studies*.  
1107 *Philosophical transactions of the Royal Society of London. Series B, Biological*  
1108 *sciences* 362:175–86.
- 1109 Zucol, A. F. 1996. Microfitolitos de las Poaceae Argentinas: I. Microfitolitos foliares de  
1110 algunas especies del genero *Stipa* (Stipae:Arundinoideae), de la Provincia de Entre  
1111 Rios. *Darwiniana* 34:151–172.
- 1112 Zucol, A. F. 1998. Microfitolitos de las Poaceae Argentinas: II. Microfitolitos foliares de  
1113 algunas especies del genero *Panicum* (Poaceae, Paniceae) de la Provincia de Entre  
1114 Rios. *Darwiniana* 36:29–50.
- 1115 Zucol, A. F. 1999. Fitolitos de las Poaceae Argentinas: IV. Asociación Fitolítica de  
1116 *Cortaderia Selloana* (Danthonieae: Poaceae), de la Provincia de Entre Ríos  
1117 (Argentina). *Natura Neotropicalis* 1:25–33.

1118 Zucol, A. F. 2000. Fitólitos de Poaceae de Argentina. III. Fitólitos foliares de especies del  
1119 género Paspalum (Paniceae) en la provincia de Entre Ríos. Darwiniana, nueva serie  
1120 38:11–32.

1121

1122

1123

1124

1125

1126

1127

1128

1129

1130

1131

1132

1133

1134

1135

1136

1137

1138

1139

1140

1141

1142

1143 **Tables and Figures**

1144

1145 Table 1 AMS Radiocarbon Dates from Huanchaca Mesetta

1146

<b>Lab Number</b>	<b>Material</b>	<b>Depth (cm)</b>	<b><sup>14</sup>C age (yr BP)</b>	<b>δ<sup>13</sup>C Ratio</b>	<b>Intcal 13 2 sigma (cal yr BP)</b>
UGAMS 15158	Macrofossil	17	190 ± 20	-28.8	0-289
UGAMS 17252	Bulk Sediment	58	2310 ± 25	-18.8	2211-2356
UGAMS 15264	Bulk Sediment	118	1360 ± 20	-22.9	1272-1305
UGAMS 12023	Bulk Sediment	190	2480 ± 20	-22.62	2473-2715
UGAMS 17253	Bulk Sediment	225	3365 ± 25	-20.7	3561-3689
UGAMS 17254	Bulk Sediment	277	6545 ± 30	-22.6	7422-9622
UGAMS 15159	Bulk Sediment	320	8600 ± 30	-22.8	9524-9622
UGAMS 17255	Bulk Sediment	380	11905 ± 35	-16.3	13577-13789

1147

1148

1149

1150

1151

1152

1153

1154

1155

1156

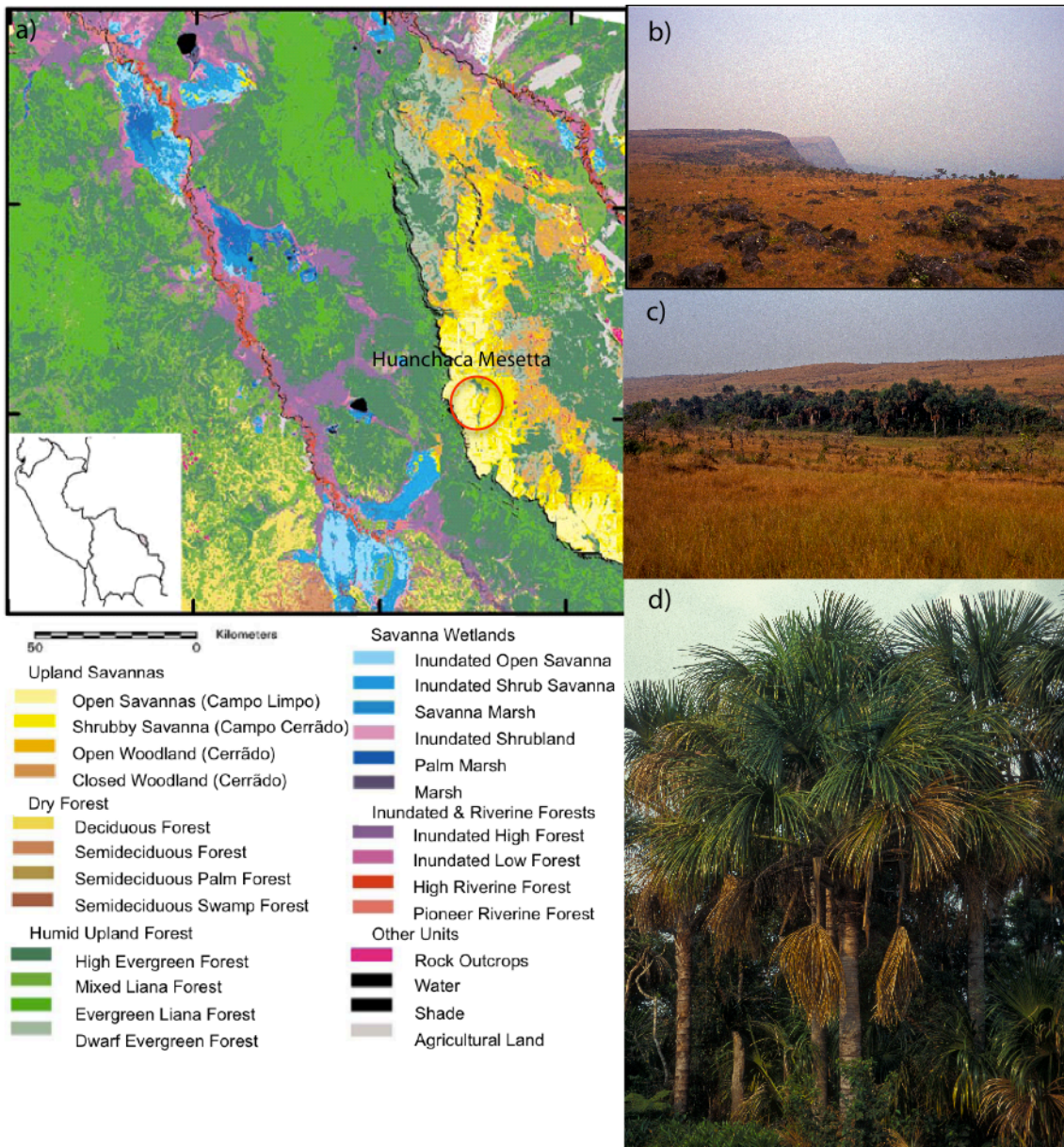
1157

1158

1159

1160

1161



1162

1163

1164

Figure 1 Huanchaca Mesetta study site a) vegetation map of Noel Kempff Mercado National Park (NKMNP) modified from Killeen et al. 1998, b) view from a top Huanchaca Mesetta, c) Huanchaca Mesetta palm swamp, d) mono-specific stand of *Mauritia flexuosa*. Photos by F. Mayle.

1165

1166

1167

1168

1169

1170

1171

1172  
1173  
1174  
1175  
1176  
1177  
1178  
1179  
1180  
1181  
1182  
1183  
1184  
1185  
1186  
1187  
1188  
1189  
1190  
1191  
1192  
1193  
1194  
1195  
1196  
1197  
1198  
1199  
1200  
1201  
1202  
1203  
1204  
1205  
1206  
1207  
1208  
1209  
1210  
1211  
1212  
1213  
1214  
1215  
1216  
1217

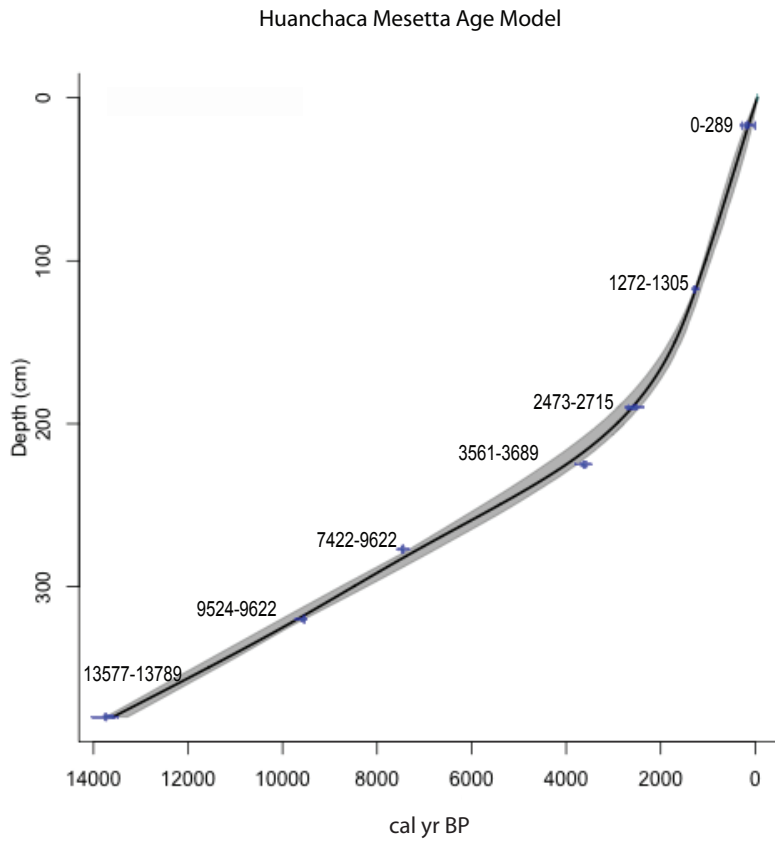


Figure 2 Clam age-depth model for Huanchaca Mesetta. Grey bars represent 2 sigma error.

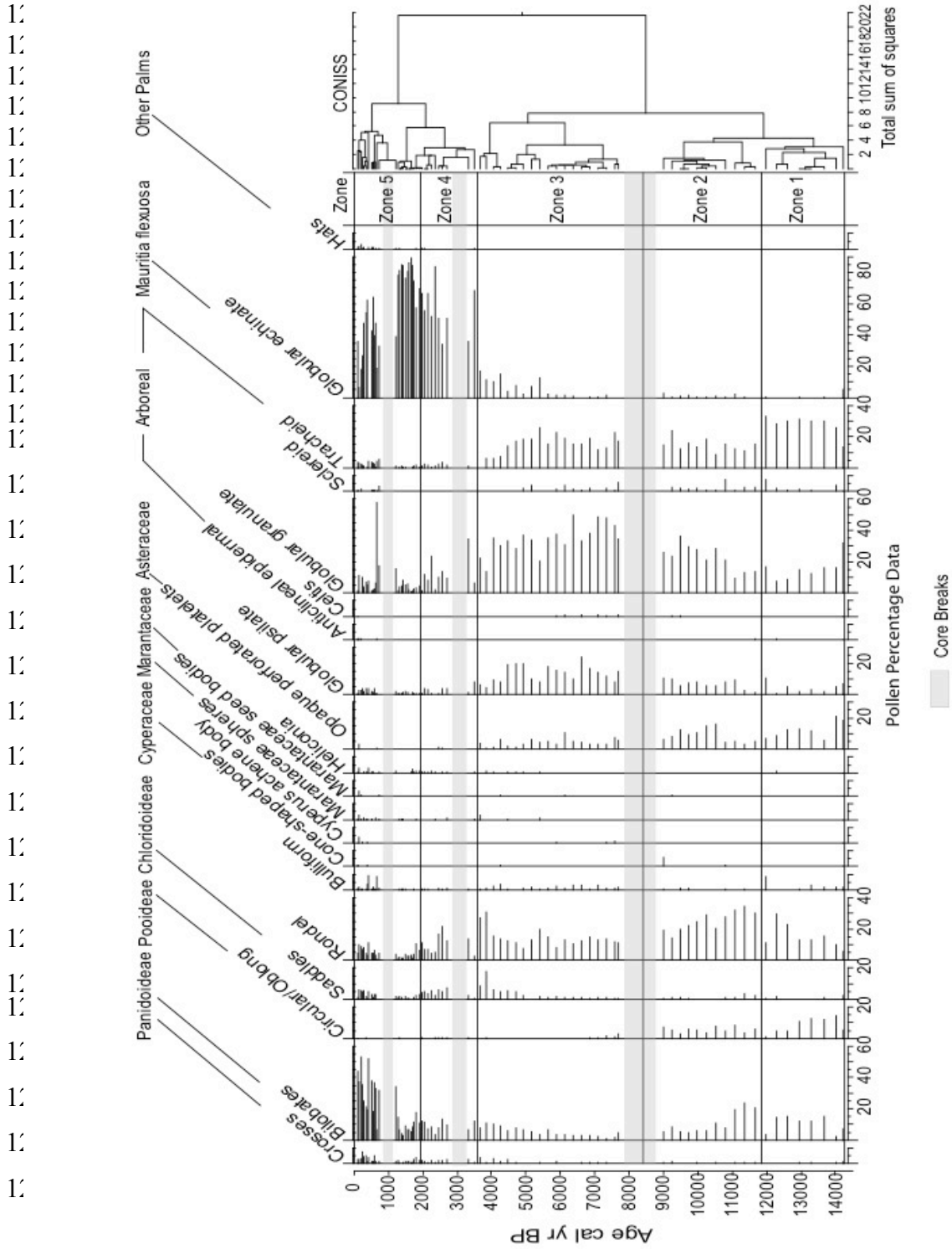
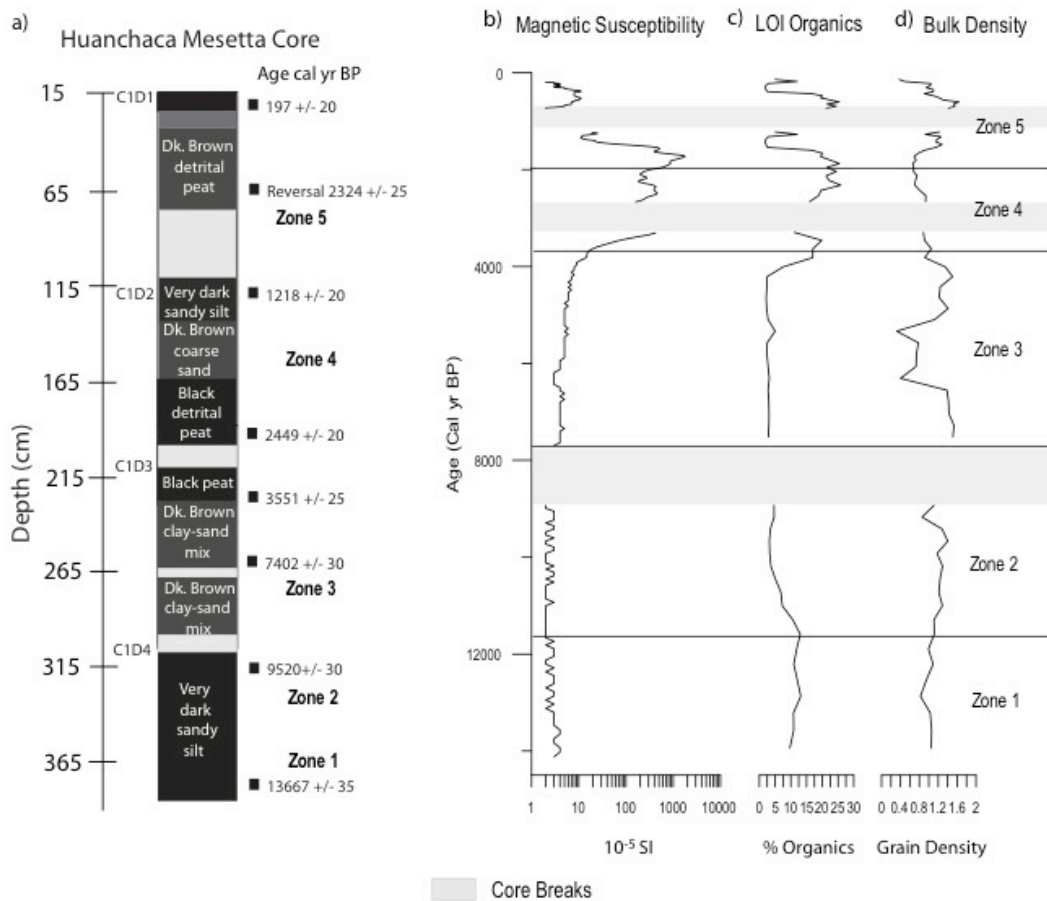


Figure 3 Huanchaca Mesetta phytolith data separated by zones created by constrained cluster analysis (CONISS). Grey bars indicate core breaks.





1250

1251

1252 Figure 4 Huanchaca Mesetta lithology a) lithological description of the core profile, b) magnetic susceptibility,  
 1253 c) loss on ignition (LOI), d) bulk density. Zones derived from phytolith data. Grey bars represent core breaks.

1254

1255

1256

1257

1258

1259

1260

1261

1262

1263

126

126

126

126

126

126

127

127

127

127

127

127

127

128

128

128

128

128

128

128

128

128

1294

1295

1296

1297

1298

1299

1300

1301

1302

1303

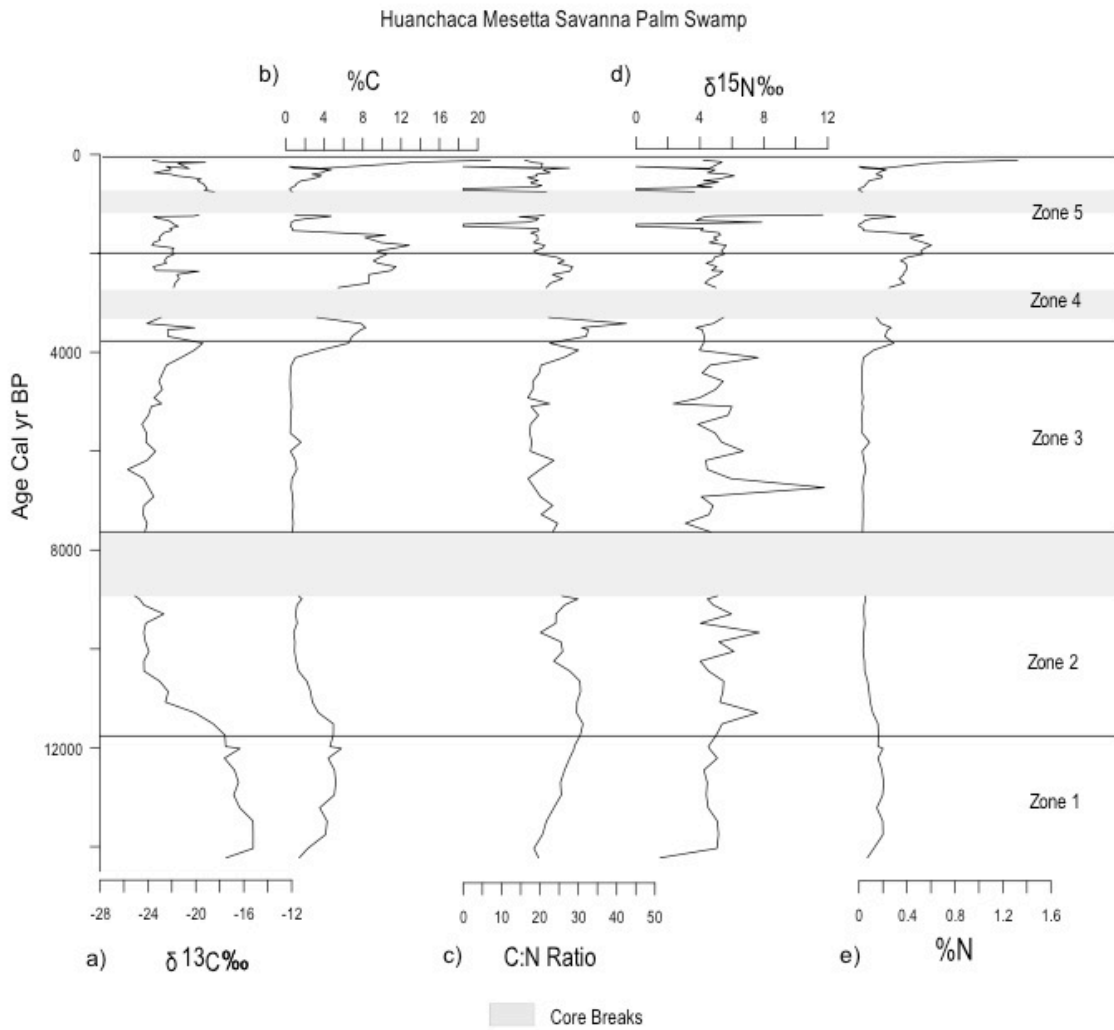


Figure 5 Huanchaca Mesetta stable isotope data a) δ13C, b) % total carbon, c) carbon to nitrogen ratio, d) δ15N, e) total %N. Zones derived from phytolith data. Grey bars indicate core breaks.

1304  
1305  
1306  
1307  
1308  
1309  
1310  
1311  
1312  
1313  
1314  
1315  
1316  
1317  
1318  
1319  
1320  
1321  
1322  
1323  
1324  
1325  
1326  
1327  
1328  
1329  
1330  
1331  
1332  
1333  
1334  
1335  
1336  
1337  
1338  
1339  
1340  
1341  
1342  
1343  
1344  
1345  
1346  
1347

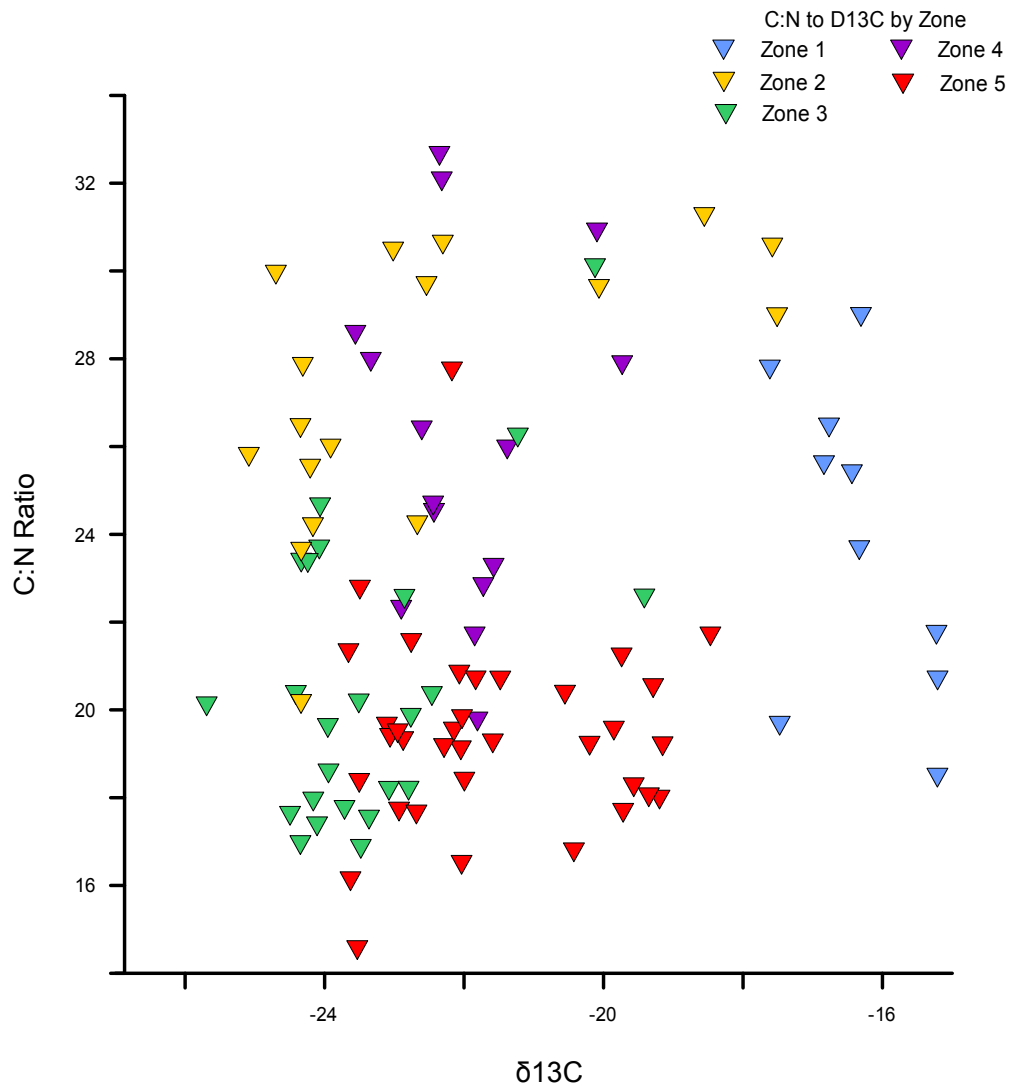


Figure 6 C:N ratio to δ13C stable isotopes by zones determined from phytolith data.

1348  
 1349  
 1350  
 1351  
 1352  
 1353  
 1354  
 1355  
 1356  
 1357  
 1358  
 1359  
 1360  
 1361  
 1362  
 1363  
 1364  
 1365  
 1366  
 1367  
 1368  
 1369  
 1370  
 1371  
 1372  
 1373  
 1374  
 1375  
 1376  
 1377  
 1378  
 1379  
 1380  
 1381  
 1382  
 1383  
 1384  
 1385  
 1386  
 1387  
 1388  
 1389  
 1390  
 1391  
 1392  
 1393

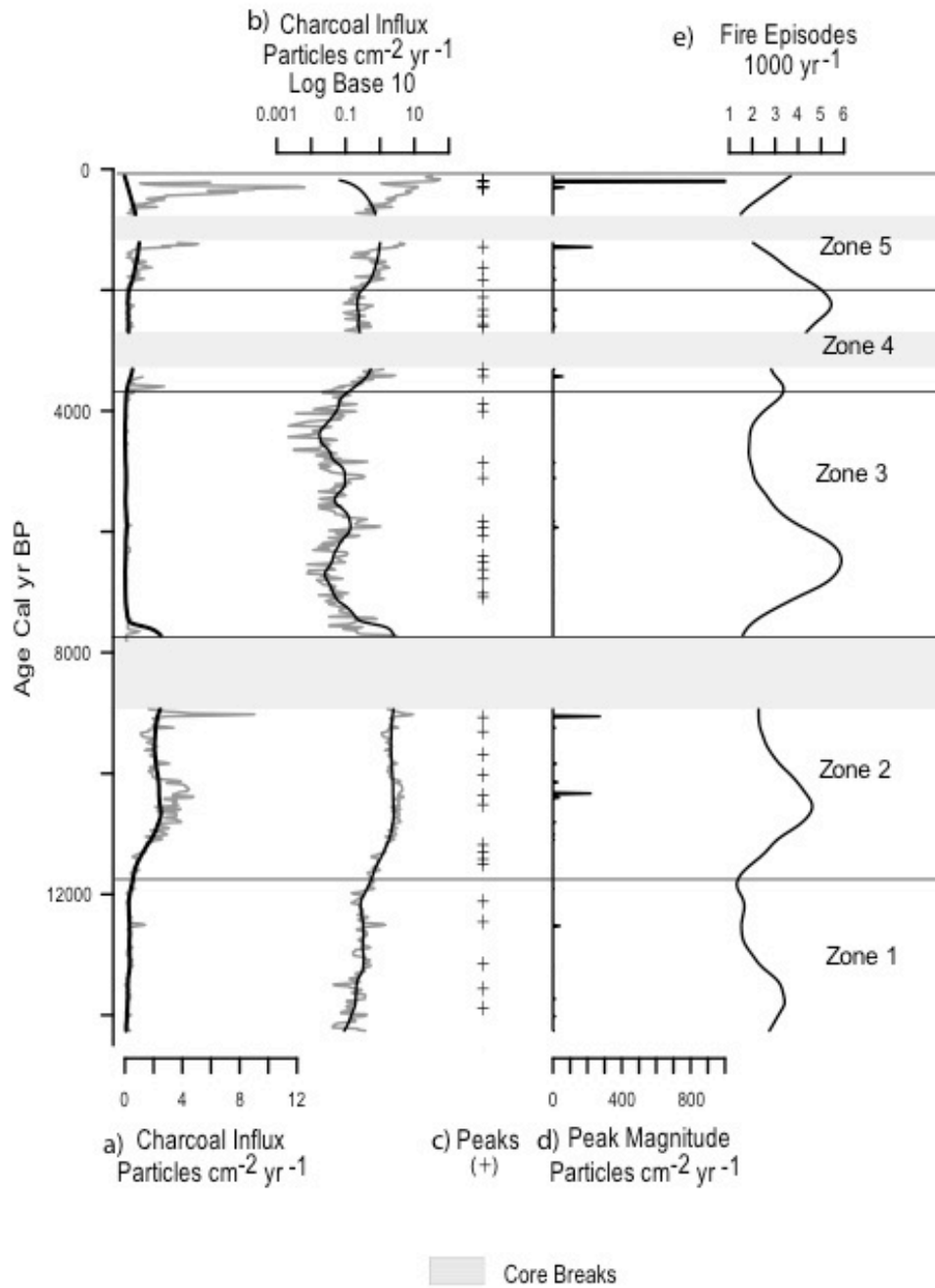


Figure 7 Huanchaca Mesetta charcoal data a) charcoal influx in grey, black background, b) charcoal influx log base 10 in grey, black background, c) peaks indicated by crosses, d) peak magnitude, e) fire episodes per 1000 years. Zones derived from phytolith data. Grey bars indicate core breaks.

1394  
 1395  
 1396  
 1397  
 1398  
 1399  
 1400  
 1401  
 1402  
 1403  
 1404  
 1405  
 1406  
 1407  
 1408  
 1409  
 1410  
 1411

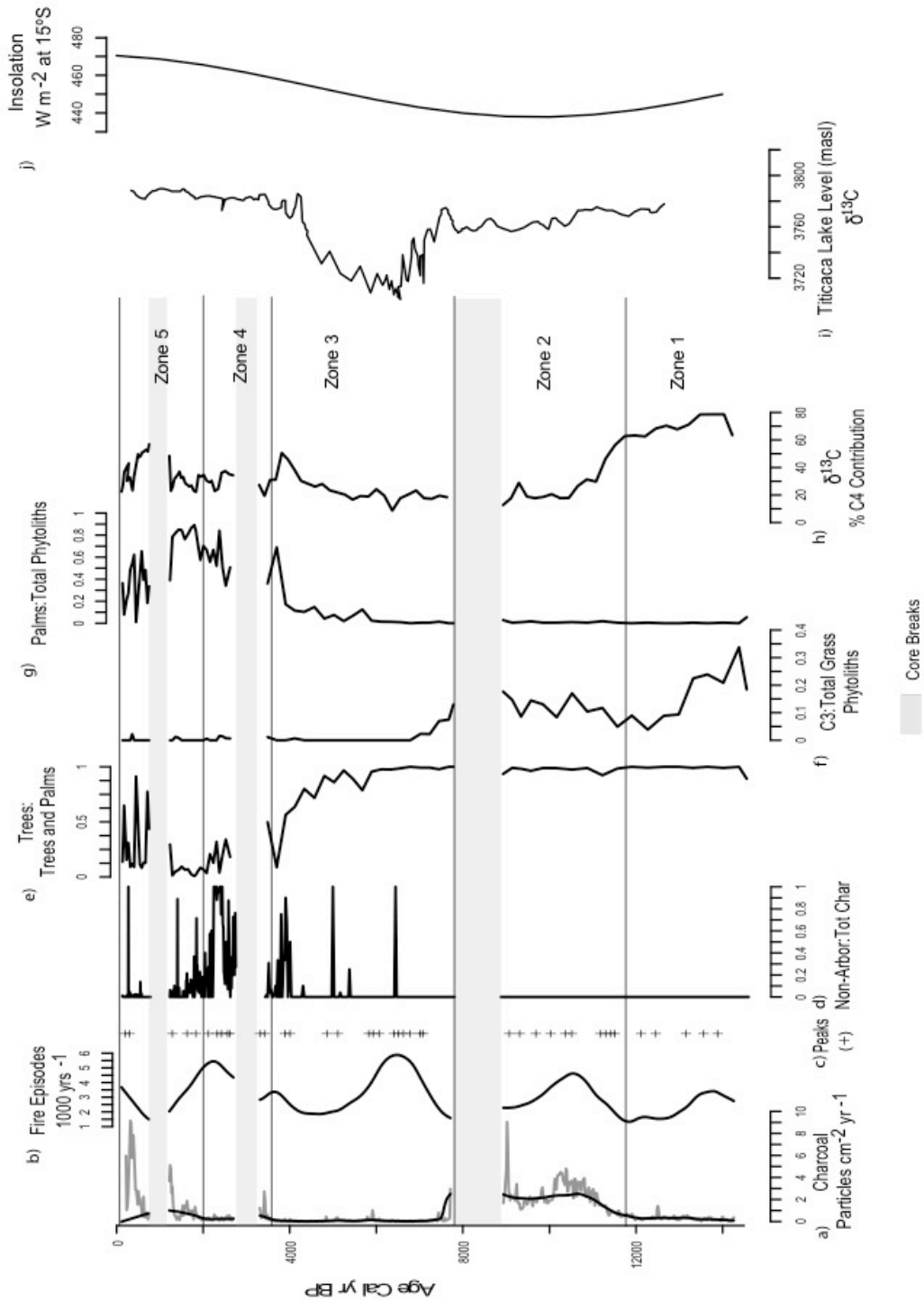


Figure 8 Huanchaca Mesetta summary figure a) charcoal influx in grey, black background, b) fire episodes per 1000 yr, c) peaks indicated by crosses, d) ratio of non-arboreal to total charcoal, e) ratio of trees to trees and palms, f) ratio of C3 to total grasses, g) ratio of palms to total phytoliths, h) % C4 contribution, i) lake level of Titicaca in meters above sea level, j) insolation at  $15^\circ\text{S}$ . Zones derived from phytolith data. Grey bars indicate core breaks.